NAVAL POSTGRADUATE SCHOOL

MONTEREY, CALIFORNIA

THESIS

LIDAR POINT CLOUD AND STEREO IMAGE POINT CLOUD FUSION

by

Paul L. Basgall

September 2013

Thesis Advisor: Fred A. Kruse
Second Reader: R.C. Olsen

Approved for public release; distribution is unlimited

THIS PAGE INTENTIONALLY LEFT BLANK

1. AGENCY USE ONLY (Leave blank)	2. REPORT DATE September 2013	3. REPORT TYPE AND DATES COVERED Master's Thesis	
4. TITLE AND SUBTITLE LIDAR POINT CLOUD AND STEREO IMAGE POINT CLOUD FUSION		**5. FUNDING NUMBERS**	
6. AUTHOR(S) Paul L. Basgall			

7. PERFORMING ORGANIZATION NAME(S) AND ADDRESS(ES)
    Naval Postgraduate School
    Monterey, CA 93943-5000
		8. PERFORMING ORGANIZATION REPORT NUMBER	

9. SPONSORING /MONITORING AGENCY NAME(S) AND ADDRESS(ES) N/A		**10. SPONSORING/MONITORING AGENCY REPORT NUMBER**	

11. SUPPLEMENTARY NOTES The views expressed in this thesis are those of the author and do not reflect the official policy or position of the Department of Defense or the U.S. Government. IRB Protocol number ____NA____.

12a. DISTRIBUTION / AVAILABILITY STATEMENT Approved for public release; distribution is unlimited	12b. DISTRIBUTION CODE

13. ABSTRACT (maximum 200 words)
The advent of Light Detection and Ranging (LiDAR) point cloud collection has significantly improved the ability to model the world in precise, fine, three-dimensional details. The objective of this research was to demonstrate accurate, foundation methods for fusing LiDAR data and photogrammetric imagery and their potential for change detection. The scope of the project was to investigate optical image to LiDAR registration methods, focusing on several dissimilar image types including Optical Bar Camera (OBC), high resolution aerial frame, and WorldView 1 satellite with varying LiDAR point densities. An innovative optical image to LiDAR data registration process was established. This approach was demonstrated for one image type using the rational polynomial coefficients (RPC) representation of the panoramic math model improving accuracy from 1.9 m to 0.5 m root mean square (RMS) error. Comparison of stereo imagery point cloud data to the LiDAR point cloud using a 90% confidence interval highlighted changes that included small scale (< 50cm), sensor dependent change and large scale, new home construction change. This research also proposed a fused LiDAR and stereo image base layer as the foundation for further LiDAR/image fusion.

14. SUBJECT TERMS LiDAR, Photogrammetry, Fusion, Accuracy			15. NUMBER OF PAGES 81
			16. PRICE CODE

17. SECURITY CLASSIFICATION OF REPORT Unclassified	18. SECURITY CLASSIFICATION OF THIS PAGE Unclassified	19. SECURITY CLASSIFICATION OF ABSTRACT Unclassified	20. LIMITATION OF ABSTRACT UU

THIS PAGE INTENTIONALLY LEFT BLANK

LIDAR POINT CLOUD AND STEREO IMAGE POINT CLOUD FUSION

Paul L. Basgall
DoD Civilian, National Geospatial-Intelligence Agency
M.S., Purdue University, 1991
B.S., Fort Hays State University, 1987

Submitted in partial fulfillment of the
requirements for the degree of

MASTER OF SCIENCE IN REMOTE SENSING INTELLIGENCE

from the

NAVAL POSTGRADUATE SCHOOL
September 2013

Author: Paul L. Basgall

Approved by: Dr. Fred A. Kruse
                 Thesis Advisor

                 Dr. R.C. Olsen
                 Second Reader

                 Dr. Dan Boger
                 Chair, Department of Information Sciences

THIS PAGE INTENTIONALLY LEFT BLANK

ABSTRACT

The advent of Light Detection and Ranging (LiDAR) point cloud collection has significantly improved the ability to model the world in precise, fine, three-dimensional details. The objective of this research was to demonstrate accurate, foundation methods for fusing LiDAR data and photogrammetric imagery and their potential for change detection. The scope of the project was to investigate optical image to LiDAR registration methods, focusing on several dissimilar image types including Optical Bar Camera (OBC), high resolution aerial frame, and WorldView 1 satellite with varying LiDAR point densities. An innovative optical image to LiDAR data registration process was established. This approach was demonstrated for one image type using the rational polynomial coefficients (RPC) representation of the panoramic math model improving accuracy from 1.9 m to 0.5 m root mean square (RMS) error. Comparison of stereo imagery point cloud data to the LiDAR point cloud using a 90% confidence interval highlighted changes that included small scale (< 50cm), sensor dependent change and large scale, new home construction change. This research also proposed a fused LiDAR and stereo image base layer as the foundation for further LiDAR/image fusion.

THIS PAGE INTENTIONALLY LEFT BLANK

TABLE OF CONTENTS

THIS PAGE INTENTIONALLY LEFT BLANK

LIST OF FIGURES

THIS PAGE INTENTIONALLY LEFT BLANK

LIST OF TABLES

THIS PAGE INTENTIONALLY LEFT BLANK

LIST OF ACRONYMS AND ABBREVIATIONS

AGL	Above Ground Level
ASCII	American Standard Code for Information Interchange
CC	Cloud Compare (Software)
CM	Centimeter
DEM	Digital Elevation Model
DSM	Digital Surface Model
DTM	Digital Terrain Model
FT	Feet
GSD	Ground Sample Distance
KM	Kilometer
LiDAR	Light Detection and Ranging
M	Meter
MSL	Mean Sea Level
NASA	National Aeronautics and Space Administration
NITF	National Imagery Transformation Format
OBC	Optical Bar Camera
QTM	Quick Terrain Modeler (QT Modeler) (Software)
RMS	Root Mean Square (Error)
TIF	Tagged Image Format
3D	Three Dimensional
TIN	Triangular Irregular Network

THIS PAGE INTENTIONALLY LEFT BLANK

ACKNOWLEDGMENTS

THIS PAGE INTENTIONALLY LEFT BLANK

I.   INTRODUCTION

Light Detection and Ranging (LiDAR) uses the measurement of timed light pulses to determine elevation differences. It produces "point clouds" of 3D data of varying density depending on the light source and interaction with the Earth's surface. LiDAR point cloud data have an outstanding ability to represent and portray topography, building structures, and foliage with precise, fine, three dimensional details. (Shan & Toth, 2009) The precision required for Light Detection and Ranging (LiDAR) point cloud data to successfully model the earth's surface and features is an open question. The goals of LiDAR measurements are similar to those of Photogrammetry.   In Photogrammetry, the objective is to extract precision three-dimensional representations of the earth's surface using analysis of parallax in stereo images. Even when viewed as photographs, photogrammetric images can appear precise because of the many fine and structured details that are visible and interpreted. LiDAR uses direct measurement of distances with respect to known ground control to determine point clouds that can be further analyzed to generate Digital Surface Models (DSM) or Digital Elevation Models (DEM).The nature of these two data sets makes them ideal for improved 3D representation of surfaces. To successfully accomplish this, however, the precision and inherent errors of each dataset need to be well understood.

It is common for LiDAR point cloud data and Photogrammetric quality imagery (mono and stereo) to be collected at different times over an area of interest. This difference in collection times can span several months to years. This fact makes co-registration and fusion challenging.

This research demonstrates the processes and results of fusing LiDAR point cloud data with photogrammetric imagery and derived stereo photogrammetric image point cloud data. The process highlights innovative techniques of registering Optical imagery to LiDAR data. In addition, the process demonstrates the improved registration accuracy when Rational Polynomial Coefficients (RPC) support data are used in place of the rigorous panoramic model for the Optical Bar Camera (OBC). Once the stereo optical imagery are coincident with the LiDAR data, fusion of optical imagery with LiDAR point

cloud data and fusion of stereo image derived point cloud data and LiDAR point cloud data can be accomplished.

We usually think about data fusion as a resource to answer a specific question or as a tool to tackle a specific problem. Data fusion can also be a means to create a new data set that is more readily exploitable. Several examples of using data fusion to create a more useable dataset exist. For example, the fusion of multispectral and panchromatic imagery is used to create a "pan-sharpened" or "resolution merge" image (Pohl & Van Genderen, 1998). Usually the multispectral image is lower resolution than the panchromatic image and the goal is to create a true color image from the multispectral image and then increase the resolution of this true color image by using the panchromatic image in a sub-pixel sampling process. This process has become so common that we often do not think about it as a data fusion process. Pan-sharpening imagery is an elegant example of how fusion of data sets can make a new data set that is more useable and ready for exploitation.

Taking the above example a step further, elevation data can used to create an orthophoto of the pan-sharpened image. This three source data fusion process of ortho-rectifying pan-sharpened color imagery creates a base layer of imagery that can be map quality and useable for precise feature extraction. We exploit the results of this three source fusion process every day when we open Google Earth™ or Yahoo Maps™.

The purpose of these examples was to show how geospatial data can be fused to create more useable and exploitable data sets. This fusion process can extend into other remote sensing phenomenologies such as LiDAR and Hyperspectral Imagery, Radar and Optical Imagery, and LiDAR and Optical imagery. The focus of this research was to study the results of fusing LiDAR point cloud data with Optical imagery and Stereo Optical imagery derived point cloud data.

II.   BACKGROUND

A.   HISTORY OF THE PROBLEM

LiDAR point cloud data can contain a lot of information in 3D space. If dense enough, this can be very useful at the individual feature level and can provide realistic views that can be rotated and viewed from many angles (Figure 1).
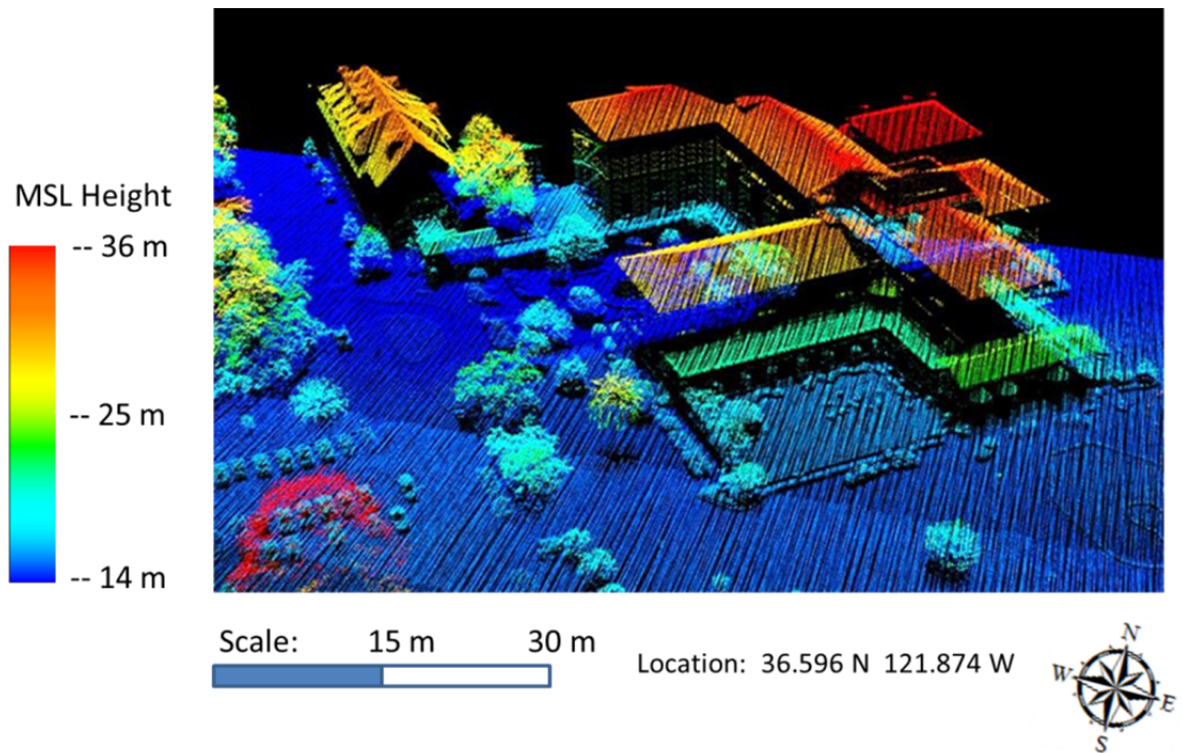
Figure 1.   LiDAR point cloud data view showing individual 3D feature level
information. Individual points are color coded by
Mean Sea Level (MSL) height.

The application of laser ranging and point cloud collection has exploded in the last decade. Close range modeling, terrestrial navigation, and airborne topography are varied examples of problems that continue to drive a need for precision LiDAR point cloud data. The fundamentals of using a laser to collect ranging or distance information in large volume apply to many 3D knowledge problems.

The history of LiDAR and photogrammetry fusion shows that many individuals with diverse interests are studying this problem. Experts from the Computer Vision community, Photogrammetry community, and LiDAR community all have an interest in solving the problems of LiDAR and imagery fusion (Kaminsky et al., 2009; Schenk et al., 2001; Rodarmel et al., 2006). After comprehensive study, these diverse disciplines show significant overlap and the problems to be solved are similar. No matter which one of these disciplines chosen, rapid collection of precision point cloud data and extraction of the 3D information content of that data are the goals.

Registering LiDAR collected point cloud data to optical imagery is not as easy as it sounds because point cloud data contains discrete points that are not easy to precisely locate on an optical image. For instance, on an optical image with the proper resolution, the corner of a sidewalk or building or roof top can be precisely identified and measured. With LiDAR point cloud data, the exact corner of a building usually does not contain a collected point. This presents a dilemma for the registration of these two data sets.

Two prevailing methods have been developed to overcome this registration dilemma (Mishra & Zhang, 2012). The first method uses derived edges from both data sets and attempts to match them up. The second method uses the LiDAR derived intensity image and DEM data to control the optical image.

Computer Vision solutions to this fusion problem have grown in popularity. Many reports elaborate on how computer vision multi-image matching has stepped up in place of photogrammetry to build point clouds (Leberl et al., 2010). One Computer Vision approach to the problem is to build the point cloud from numerous overlapping images in an arbitrary image model space and then align this point cloud to imagery through classic point, edge, and homogeneous area matching (Kaminsky et al., 2009).

While Computer Vision solutions are new and attractive, they rely heavily on image content such as building structures and roads that have strong edges and features to perform image and point cloud matching . The idea of using linear features for matching is also prevalent in the photogrammetry community as it has been successfully implemented in image to image matching routines (Habib, Ghanma, & Kim, 2005). A

quick visualization of an optical image and LiDAR point cloud shows the strong edges of both data sets that would make ideal matching features (Figure 2).
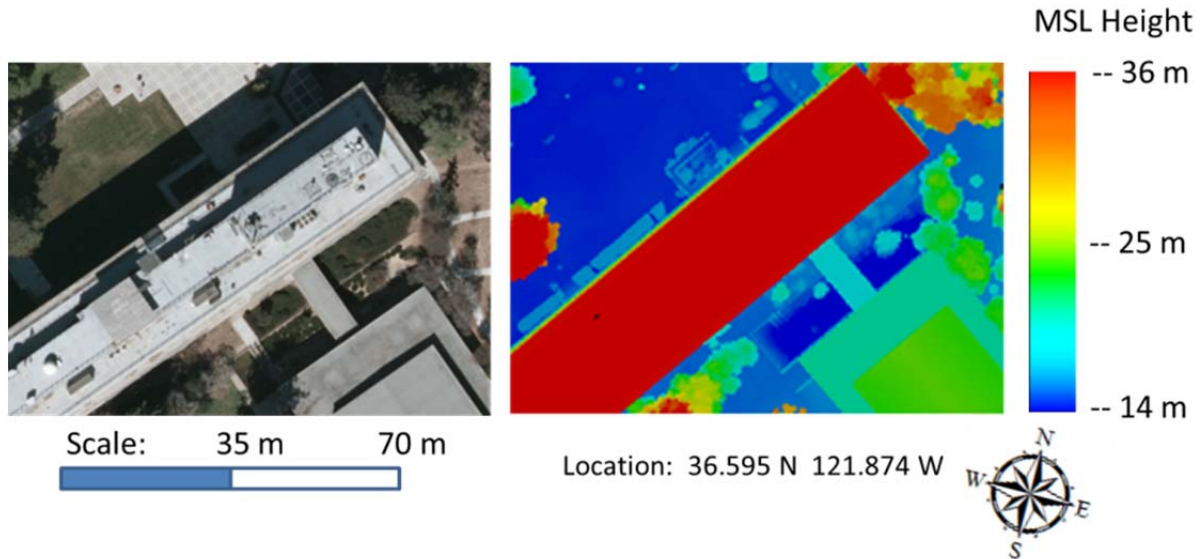
Figure 2.   Side-by-side view of a high resolution color frame image (left) and top view of a LiDAR point cloud (right) highlighting linear edge features ideal for automatic registration.

Areas where topography is being derived, unfortunately, do not always contain urban structure, and tend to be very homogeneous in image content. As a result, topographic and mapping applications tend to lean toward using the intensity image and LiDAR derived Digital Elevation Model (DEM) as a reference base. This solution for registration is not popular, however, because it is not well suited for automation (Mishra & Zhang, 2012).

One registration approach encountered is to create two images from the LiDAR data (Habib, Ghanma, & Kim, 2005). One image is the traditional intensity image and the second image is the DEM represented as a "range" image. This does not seem very accurate though because the height value is fixed for any given sub-pixel location. A better approach would be to interpolate a height value between the DEM points.

Many traditional photogrammetry researchers have recognized the mutual benefits that a photogrammetric derived point cloud and a LiDAR point cloud can

provide (White et al., 2013; Habib et al, 2008). The problem of fusing LiDAR data and photogrammetric imagery becomes much more complex when registering large-scale imagery and attempting to create true orthophotos (Habib et al, 2008). True orthophotos are different than a terrain corrected orthophoto. True orthophotos use detailed 3D feature information to stand buildings up. In the typical terrain corrected orthophoto, buildings and tall features will still retain the perspective view from the photogrammetric image often showing lean away from the center of the image. The Digital Surface Model (DSM) can be more completely described with the fusion of the LiDAR point cloud and stereo point cloud, resulting in better representation of the 3D environment. This improved representation of the 3D environment can produce more precise true orthophotos.

Outside of the urban environment, forest management has started to engage the utility of LiDAR point cloud data and how it can be used with the more traditional aerial photogrammetric practices today (White et al., 2013). The partial tree canopy penetration capabilities of LiDAR help to establish tree height and tree maturity. Also, the underlying Digital Terrain Model (DTM) can be created from the LiDAR data to understand water drainage and road access. These data can then be fused with photogrammetric and multispectral image derived tree species and tree health information, resulting in a complete model of the forest inventory.

LiDAR collected point clouds and stereo-image-derived point clouds can also be used for change detection (Schenk & Csatho, 2003), which is one of the focuses of this research. The derived data from each sensor can be used to investigate catastrophic change that may have occurred as a result of a natural or man-made disaster. Rapid assessment of destructive events allows local emergency response and local government personnel to make better actionable decisions.

Another concept in LiDAR and optical image fusion is the ability to use accurate stereo imagery to assess the quality of LiDAR point clouds. In layman's terms, this is sometimes known as "draping" the point cloud over the stereo images. In photogrammetric practice, a technique called "back-projection" is used, which takes the X,Y,Z coordinate of each point in the point cloud and computes the corresponding image

coordinates for each point (Schenk, Seo, & Csathó, 2001). The points can then be viewed in stereo, comparing the point locations to actual surface features. If the stereo images have a reported accuracy, then this technique can be used to establish or verify LiDAR point cloud accuracy. This technique is frequently used for Digital Elevation Model (DEM) evaluation.

The LiDAR point cloud and single optical image fusion process is the most intriguing near term topic in terms of what it has to offer towards improved surface analysis. Standard practice for deriving precision 3D coordinates is to use accurate stereo imagery and a two-ray image measurement intersection routine. Performing a stereo measurement can be very challenging for an analyst and requires proper viewing equipment. A fused LiDAR-optical image data set allows precision computation of 3D coordinates without relying on this stereo image measurement. The process of deriving a 3D coordinate on a single image is called "single ray intersection." The single ray intersection process needs precise elevation data coincident with the single image in order to correctly intersect the image ray on the ground or object. The LiDAR data registered to the image can provide these precise elevation data for objects or ground features in the image allowing for precise 3D coordinate derivation through the single ray intersection process (Rodarmel et al., 2006).

Being able to compute precise 3D coordinates from a single image has advantages for improved exploitation. Single image exploitation can be done on a handheld device like a cell phone or tablet. The process of exploitation could be as simple as placing a cursor on a feature in the image. This research explores the LiDAR and optical image fusion process starting with the problem of image and LiDAR registration.

THIS PAGE INTENTIONALLY LEFT BLANK

III.   OBJECTIVES

The main objectives of this research was to demonstrate innovative techniques of the LiDAR point cloud and photogrammetric image registration process and to compare LiDAR point cloud and stereo photogrammetric derived point clouds, their characteristics, and precision.   This thesis also summarizes the important points of creating a fused image/LiDAR data set for improved exploitation.

THIS PAGE INTENTIONALLY LEFT BLANK

IV. DATA PROCESSING METHODS, RESULTS, AND ANALYSIS

A. STUDY AREA AND DATA

1. Haiti LiDAR and Optical Bar Camera Imagery

The first study area was chosen near Port-au-Prince, Haiti because both LiDAR data and Optical Bar Camera (OBC) imagery existed as a result of support for earthquake and humanitarian relief efforts. Both data sets were collected in late January of 2010 following the 7.0 magnitude earthquake that occurred near Port-au-Prince, Haiti on January 12, 2010. A small subset of LiDAR data was selected from a larger available LiDAR database that coincided with the area of the OBC image coverage. The following map graphics show the exact location of the LiDAR subset (Figure 3).

Figure 3.   This overview map (left) and zoomed map (right) show the area in Haiti near Port-au-Prince where the LiDAR data were extracted from the OpenTopography Website. The red box in the right zoom map display highlights the location of the downloaded LiDAR data (3.4 points/m^2).

The LiDAR data collection was performed by the Center for Imaging Science at Rochester Institute of Technology (RIT) and Kucera International under sub-contract to

ImageCat, Inc. (Open_Topography, 2008). The downloaded data consisted of 28.5 million points with a density of 3.4 points/m^2. The project was funded by the Global Facility for Disaster Reduction and Recovery (GFDRR) and the data are hosted at the World Bank (www.opentopography.org). The following figure (Figure 4) shows a 3D perspective view color coded by Above Ground Level (AGL = DSM-DEM) height of the downloaded Haiti LiDAR data and displayed in Quick Terrain Modeler (QTM) (Applied_Imagery, 2004) .
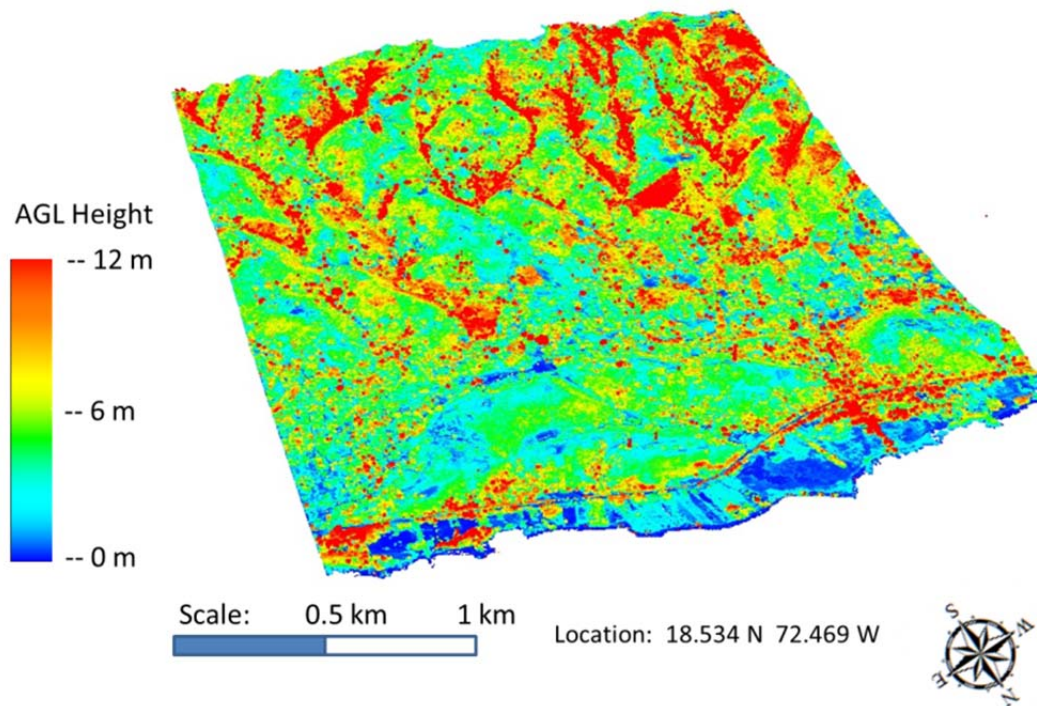
Figure 4.   Oblique view of downloaded Haiti LiDAR data color coded by
Above Ground Level (AGL) Height (in meters). This data set
contains approximately 28.5 million points.

The Optical Bar Camera (OBC) imagery is collected by the United States Air Force (UTC_Aerospace_Systems, 2013). The OBC itself is a large format calibrated panoramic camera capable of photogrammetric quality image collection. The OBC imaging mission for Haiti was performed on January 30, 2010 flying at an altitude of 42,000 feet producing an approximate Ground Sample Distance (GSD) of 0.15 meters.

The OBC imagery is film (hardcopy) based and must be digitized. The large format image is traditionally digitized using 14 micrometer pixel sizes in 15 degree, 8-bit TIF or NITF format segments. One segment was chosen that covered the LiDAR test area (Figure 3 and Figure 5). This OBC segment is centered on the +15 degree mark of the full (-72 to +72 degree) panoramic image and was further clipped to eliminate the water area as no control points could be selected in that area.
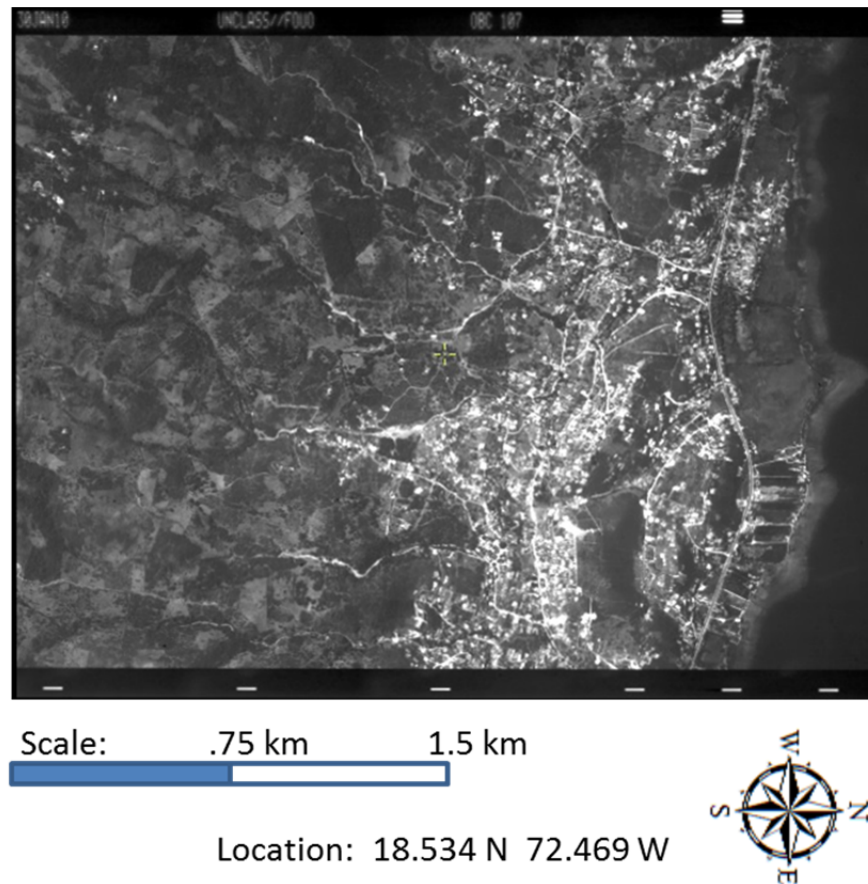
Figure 5.   Segmented piece of OBC imagery in Haiti near the LiDAR coverage area. This image was further clipped to eliminate the water.

2.   NPS Campus LiDAR and High Resolution Aerial Imagery

High resolution LiDAR and optical data were recently collected over a portion of the Naval Postgraduate School campus, Monterey, California, and are included as part of this study. The LiDAR point cloud was collected in October 2012 by Watershed

Sciences, Inc. (WSI). Mounted in a Bell 206 Long Ranger Helicopter, the LiDAR data were collected at a very dense average of 30 points/m^2 using an Optech Orion C200 laser system (Watershed Sciences, 2012). The following graphic shows the location of the complete LiDAR collect over the Monterey Peninsula. A subset of this data over the NPS campus was selected as the focus of this thesis (Figure 6, Figure 7).
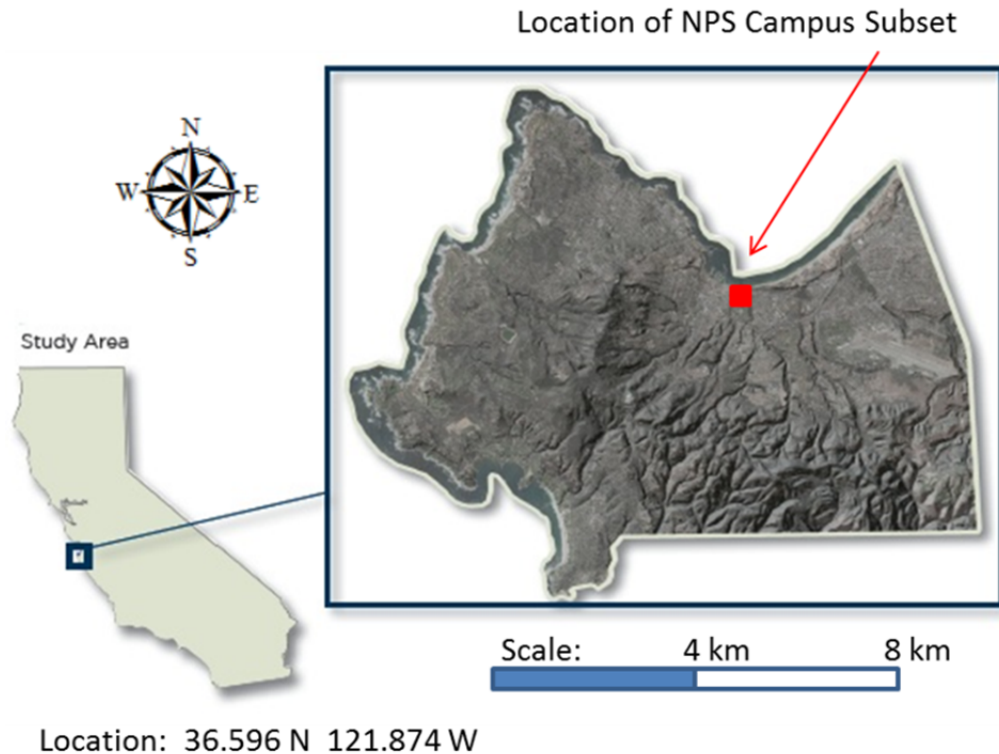
Figure 6.   Image from the Watershed Sciences Report (Watershed Sciences, 2012) showing the complete Monterey peninsula WSI LiDAR collection in October, 2012
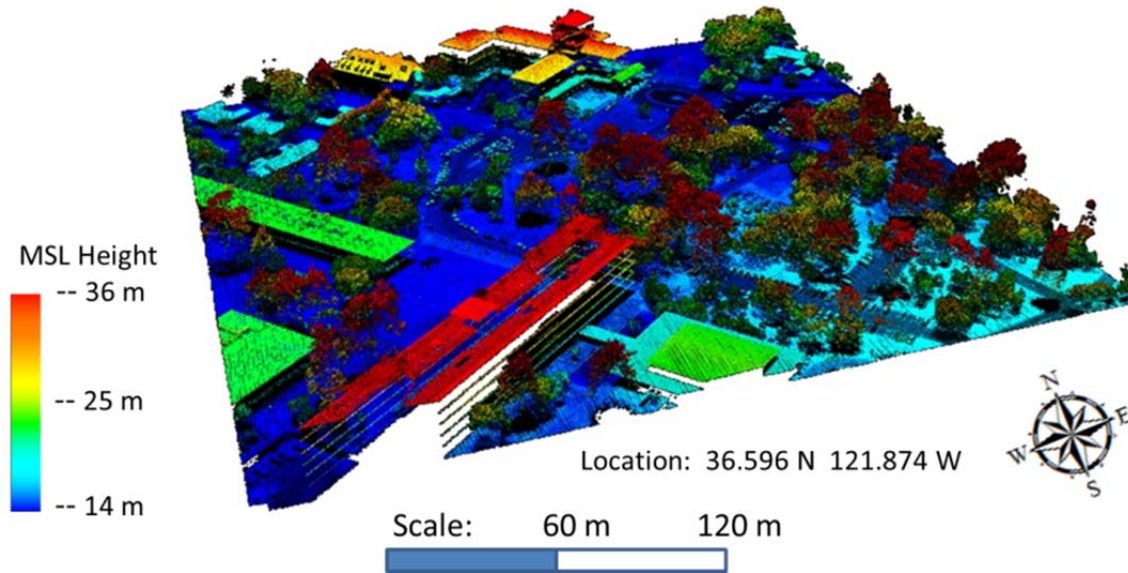
Figure 7. Selected LiDAR subset of the NPS campus. 3D Perspective view
displayed in QT Modeler software and colored by height
(internally known as tile 774)

The optical imagery was collected in stereo using a multispectral UltraCam Eagle, 260 megapixel camera manufactured by Vexel Corporation, a Microsoft subsidiary. The color imagery scans were collected at 450m flying height producing high resolution 15cm pixels (Watershed Sciences, 2012). The following diagram (Figure 8) shows the footprints of the single images, the amount of overlap between successive images, and the amount of sidelap between the strips. The NPS campus area is near the center, marked by the red outline.
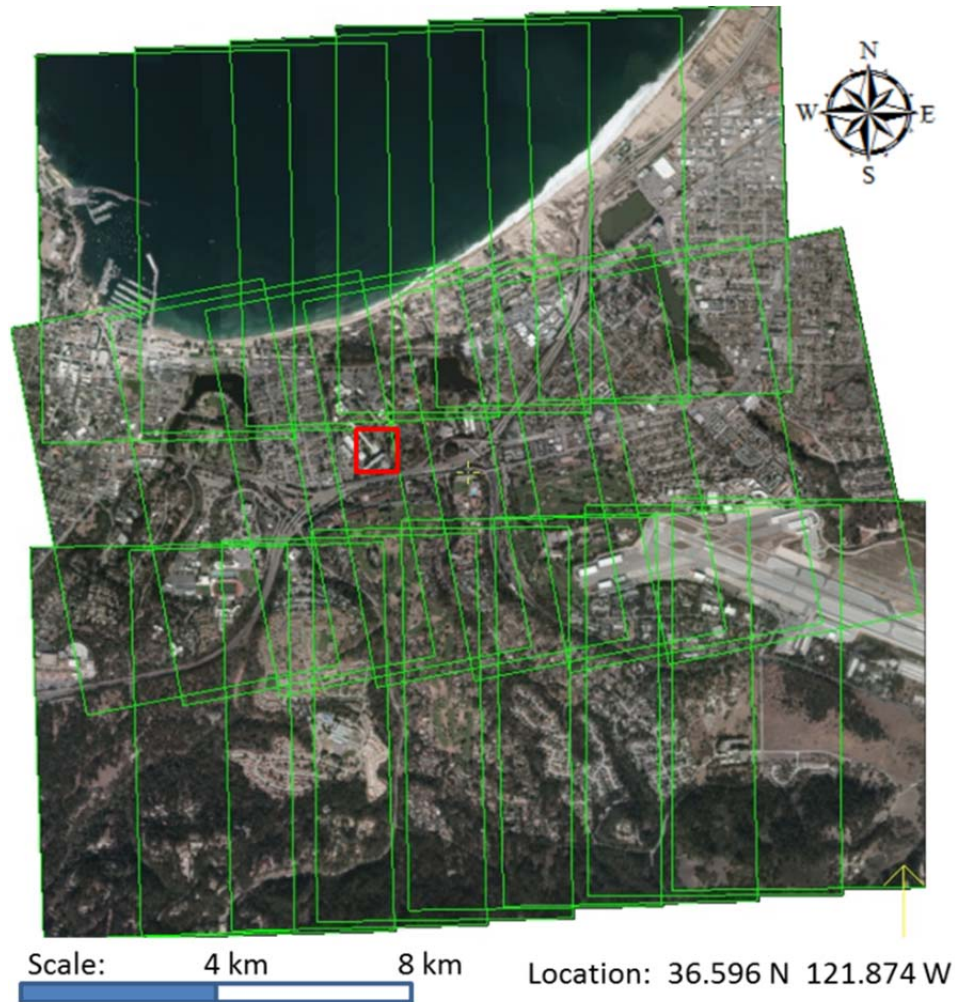
Figure 8.   UltraCam Eagle stereo image footprint coverage diagram showing overlap between images and sidelap between strips. The NPS campus area is marked by the red outline.

The imagery has very good photogrammetric quality capable of supporting precision DEM extraction. The following split screen view (Figure 9) of the UltraCam Eagle color images shows a section of the NPS campus.
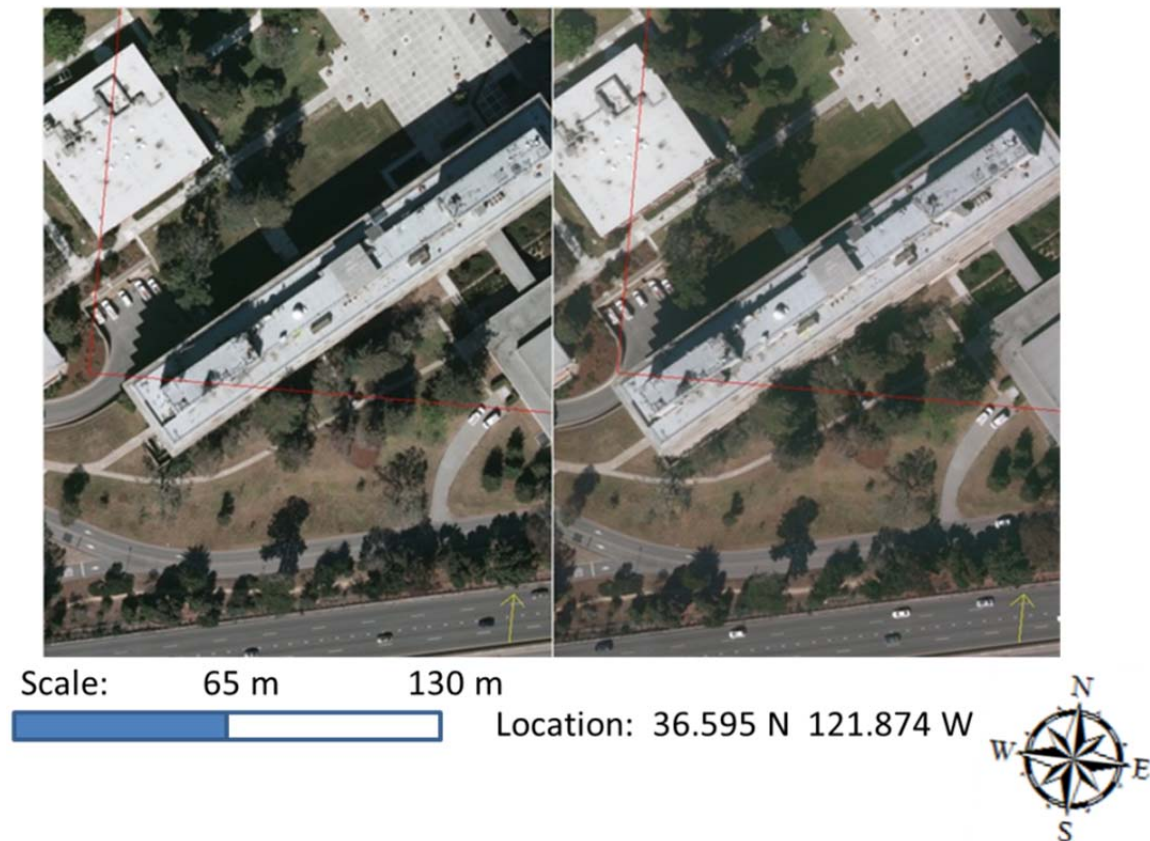
Figure 9.   Stereo images of the NPS campus shown in split screen view detailing the quality of the stereo imagery capable of precise, high resolution DEM or point cloud extraction. The red lines highlight part of the DEM extraction area.

3.   San Diego LiDAR and WorldView 1 Imagery

The third study area was chosen near Pacific Beach, California, which is just north of San Diego, California. This study area was chosen because WorldView 1 (WV1) stereo imagery was available along with LiDAR data (Open_Topography, 2008). A small subset of LiDAR data was selected and downloaded using the opentopography web site LiDAR retrieval tool. The LiDAR was collected in January 2005 by Merrick, Inc. for the City of San Diego at 1.4 points/m^2. This small subset of LiDAR data coincided with the area of the WV1 image coverage. The following map graphics (Figure 10) show the exact location of the LiDAR subset.
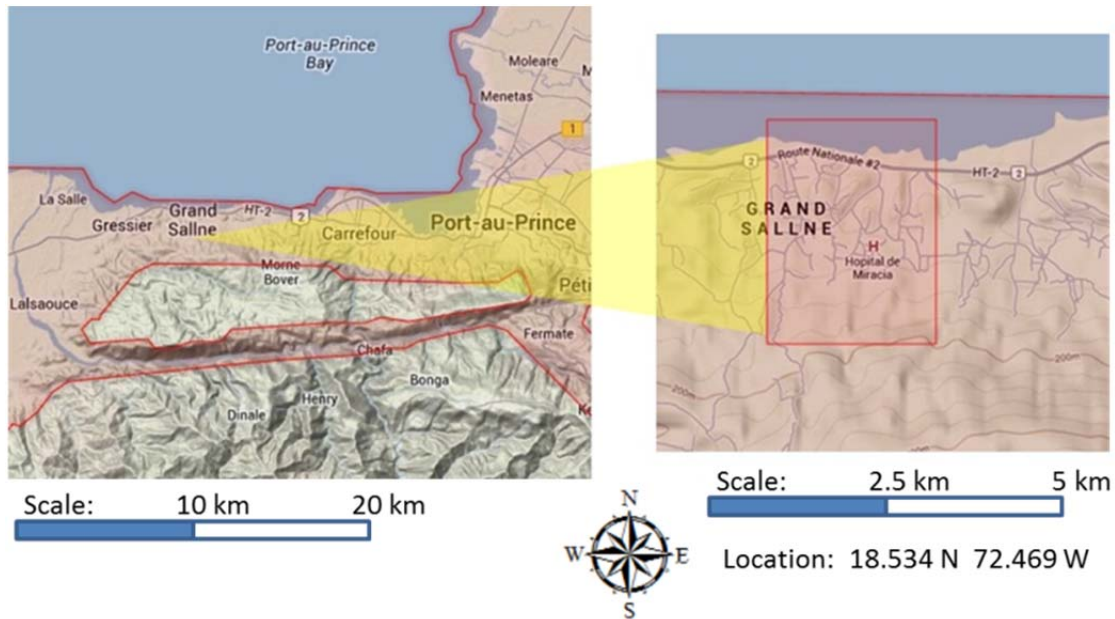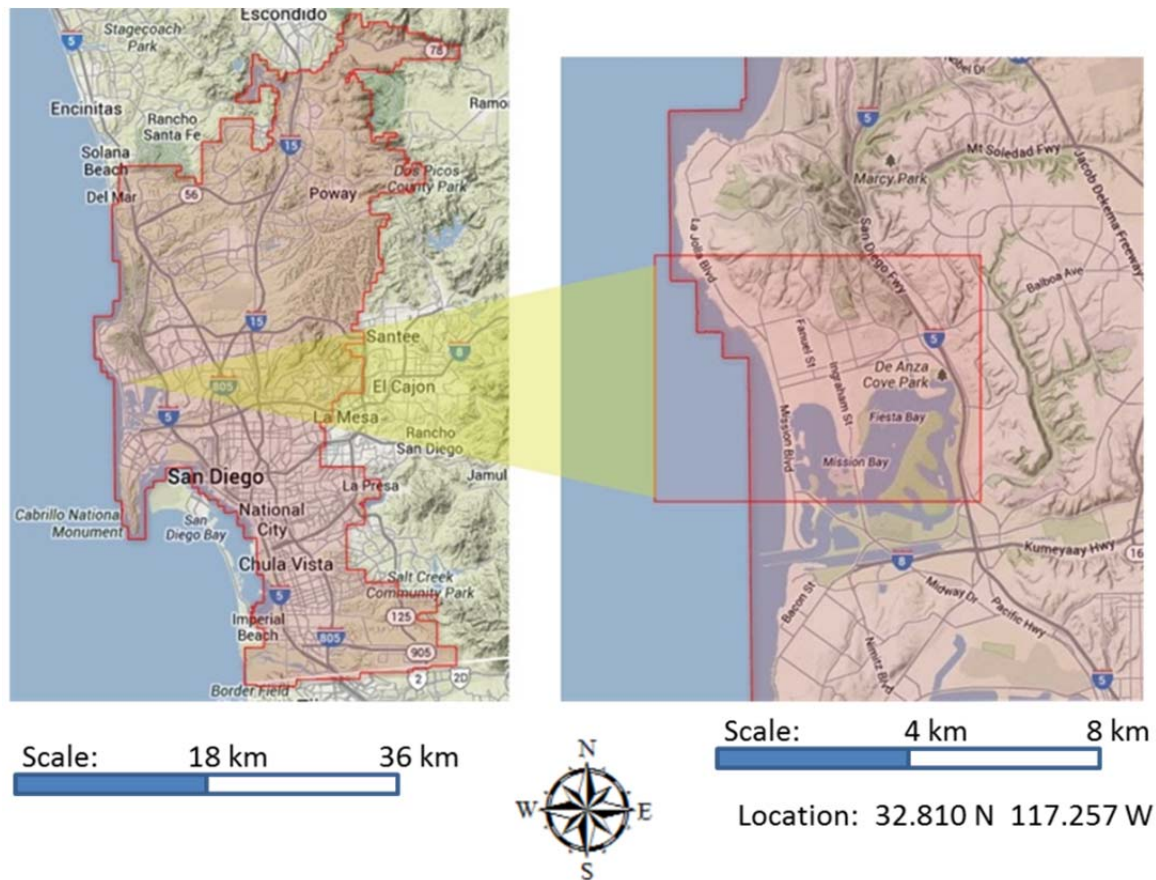
Figure 10. This overview and zoomed map display show the area in
Pacific Beach near San Diego, California where the LIDAR data were
extracted from the OpenTopography Website (Open_Topography, 2008).
The red box in the right zoom map display highlights the location of the
downloaded LiDAR data (1.4 points/m^2).
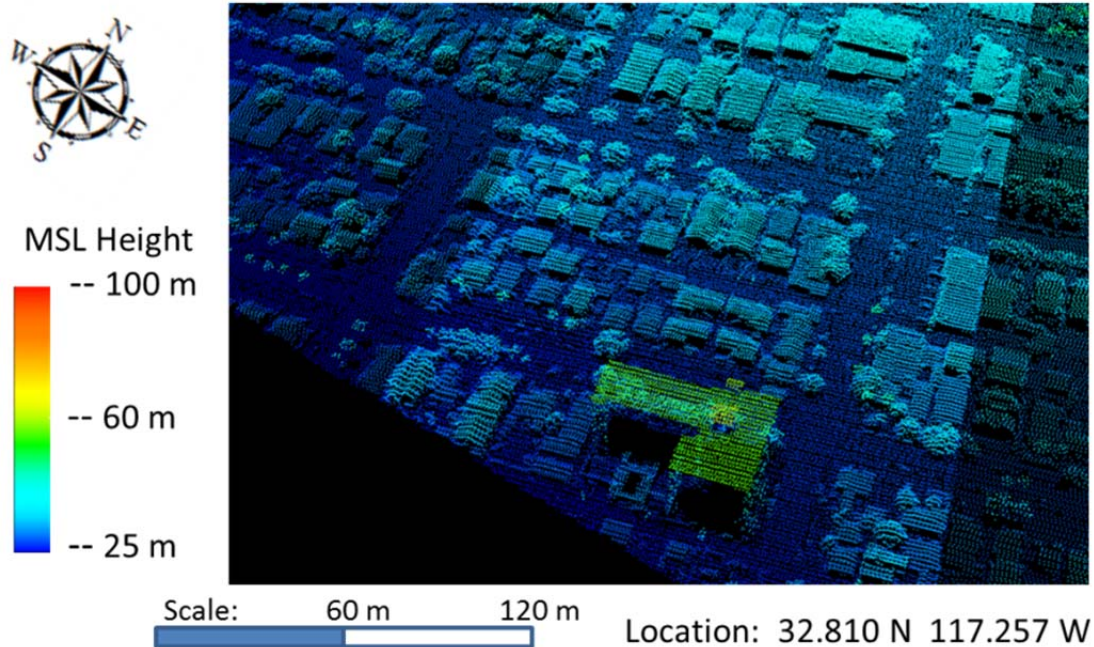
Figure 11. Colorized rendition of a zoomed in section located in the Southeast corner of the downloaded Pacific Beach LiDAR data set. The data was collected in 2005 at a 1.4 points/m^2 density.

The stereo optical imagery used in this third case study is from Digital Globe's WV1 satellite. WV1 is strictly a panchromatic (B/W) image collector with large footprints and 0.6m pixels. The images were collected as a stereo triplet—3 images consecutively. Each stereo pair image combination (1–2, 1–3, 2–3) from the WV1 triplet was used to extract a DEM using photogrammetric methods, and from these three independent DEMs, the one with the least amount of automatic correlation errors was used. The following graphic (Figure 12) shows the coverage of the WV1 stereo triplet as well as the outline of the LiDAR coverage.

Scale: 4 km 8 km Location: 32.810 N 117.257 W

Figure 12.   This image shows the large red outline of San DiegoWV1 stereo triplet coverage and a smaller interior red box that outlines the downloaded LiDAR coverage for the Pacific Beach area.

The following images (Figure 13) show a split screen view of the WV1 stereo imagery detailing the quality and perspective view of the individual images.
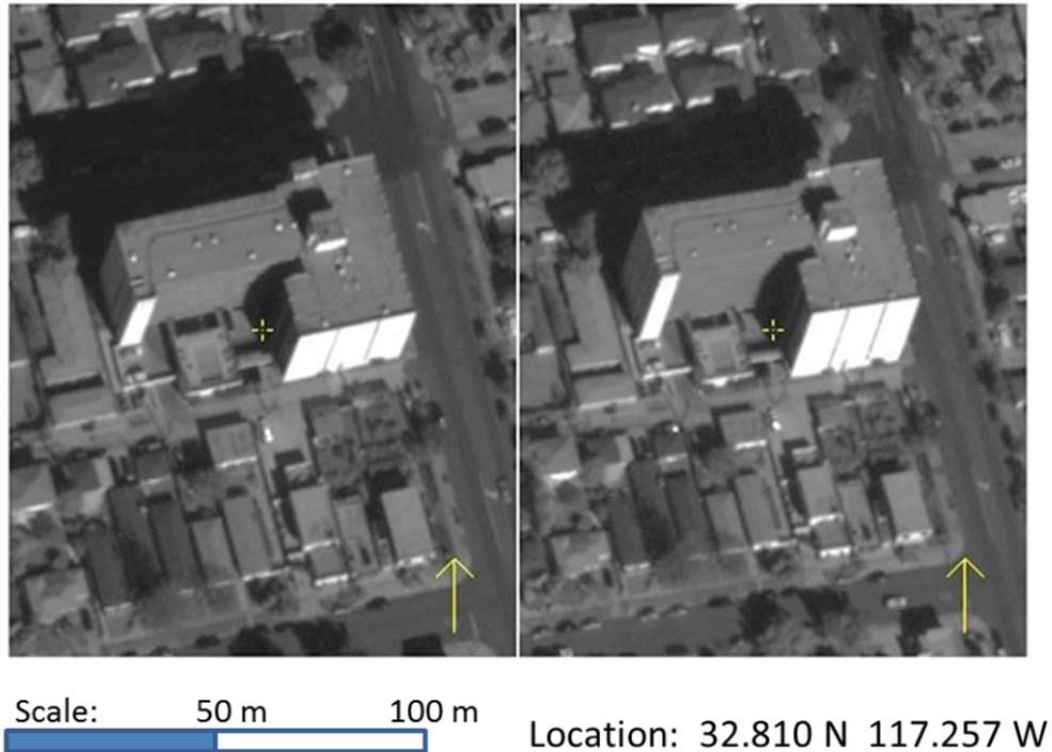
Figure 13.   WV-1 stereo image area of Pacific Beach shown in split screen view detailing the quality of the stereo imagery capable of DEM or point cloud extraction. (GSD = 0.6 meters)

B.   REGISTRATION OF OPTICAL IMAGERY TO LIDAR

This research focused on using the "Intensity Image" approach for controlling optical imagery to LiDAR (Mishra & Zhang, 2012) as opposed to the feature or edge matching approach that has been thoroughly studied by several researchers (Du, Xu, & Cao, 2009; Mishra & Zhang, 2012). In the majority of cases, the identifiable feature content of an intensity image will be sufficient enough for common points to be found between the optical image and the intensity image. It is also important to select these common points in relatively flat regions because the height value for the point selected on the intensity image will have to be interpolated from the LiDAR created TIN or DEM. If the point selection is done properly, very accurate points can be interpolated from the LiDAR data even though the selected point may not represent a real collected LiDAR point. Once collected, these precision interpolated points can be used to control the optical imagery in a triangulation process.

21

The following process flow summarizes a standard method for controlling optical imagery to LiDAR data (Table 1). This generic process was derived from similar image-to-image registration processes using the "Socet Set" software (BAE_Systems, 1990).

Generic LiDAR Control Process Flow

1. Import LiDAR data (.las file)
   A. Creating Intensity Image
   B. Creating DEM (no thinning)

2. Import Imagery to be controlled

3. Build Control Point File using Control Point Editor
   A. Locate Control Points on Intensity Image
   B. Interpolate Height using LiDAR DEM (Terrain Tracking)
   C. Capture a description of control point location (sketch)

4. Create Triangulation File
   A. Include Image and Control Point File

5. Locate and Measure each Control Point
   A. Use sketch for correct identification

6. Use Triangulation Solve to adjust Imagery

Table 1.   Generic LiDAR Control Process Flow Defined Using Socet Set

As part of this research an innovative, improved process was developed to control imagery to LiDAR (Table 2).

Improved LiDAR Control Process Flow

1. Import LiDAR data (.las file)
   A. Creating Intensity Image
   B. Creating DEM (no thinning)

2. Import Imagery to be controlled

3. Build Triangulation File
   A. Include Imagery and Intensity Image

4. Measure Common Points
   A. On LiDAR Intensity Image and Optical Imagery
   B. Point Pattern Sufficient for Image Type

5. Create Control Points from LiDAR Data Using Triangulation Solve
   A. Solve for ground point locations on intensity image
   B. Update Ground Control File
   C. Interpolate Height using LiDAR DEM
   D. Update ground control file with new height

6. Use Triangulation Solve to adjust Imagery

Table 2.   Improved LiDAR Control Process Flow Derived Using Socet Set

The improved LiDAR control process contains two enhancements. First, including all imagery in the Triangulation allows common points to be measured on all imagery in the same viewing window and allows the review of those measured points at any time before or after the triangulation solution. The capability to review points is very useful in the case of control point miss-identification. Second, by activating/deactivating images, changing weights on image parameters, and changing weights on ground control points, the triangulation solve can be used to derive ground control points in one step and then used to adjust the optical imagery in a second step. Using the triangulation solve to generate ground control also gives a triangulation report that details residuals and parameter adjustments that can be used for quality assurance.

23

1. Haiti LiDAR and Optical Bar Camera Imagery

Once the basics of registering optical imagery to LiDAR were outlined as above, the first challenging case study was to investigate the registration of Optical Bar Camera (OBC) imagery to LiDAR for the Haiti site. The registration of OBC imagery using control points is challenging. The challenging part is that the imagery were collected with an airborne panoramic camera, which introduces the complicated dynamics of the panoramic camera and, in the case of OBC, disconnected sensor positioning and orientation information. Also, OBC imagery starts out as a hardcopy film that must be digitized. Importing this scanned imagery into photogrammetric exploitation software using the correct panoramic math model and proper metadata can be tedious.

The required sensor position and orientation information is separate from the imagery and must be correctly identified and captured. Once this important data is retrieved, the values must be hand entered in required fields upon image import. The example below is from the Socet Set software (Figure 14).

Figure 14.   Socet Set panoramic camera position and orientation input page.
All data must be input by hand.

Because the scanned imagery is a segment of a full panoramic image that may occur at any degree sweep, the input roll angle of the sensor has to be changed to give the impression that the camera is pointing in that direction (Figure 15).
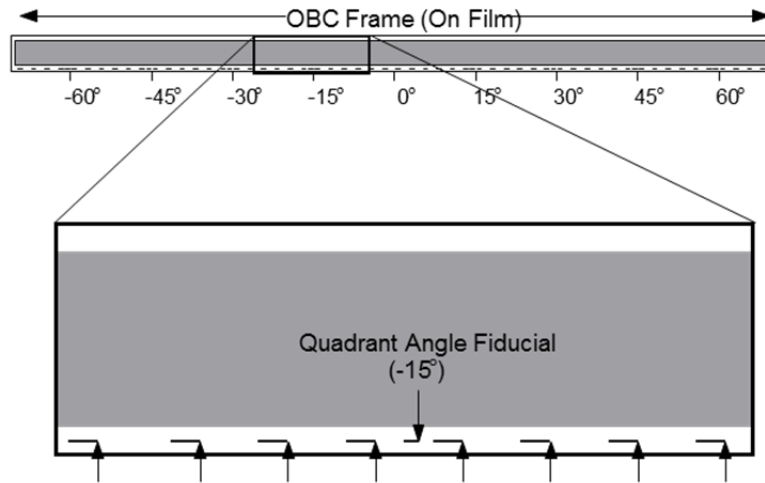
Figure 15.   Diagram of a 15 degree scanned segment of OBC film centered
at the negative 15 degree scan mark.

If the metadata are correctly input, the imagery will import properly and align to within 100 meters of absolute ground truth. In any case, this raw OBC image positioning otherwise known as "apriori positioning" requires controlling or registration for LiDAR fusion and exploitation. At this juncture, the LiDAR data are also imported, creating an intensity image and a regularly spaced gridded DEM interpolated from the LiDAR point cloud. All of the ingredients are now in place to continue the optical image to LiDAR registration process as outlined in Table 2.

The next step in the process is to measure common points between the OBC imagery and the LiDAR intensity image using an interactive point measurement function. Selecting and measuring quality common points are a skill that requires practice. The goal in optical image to LiDAR intensity image point transfer is to find small features that are clearly identifiable in both images. Also, because we need to interpolate a height value from the LiDAR DEM, the selected point should be in a relatively flat area. Figure 16 shows an example of a common selected point.

25

Figure 16. This side-by-side image display of a subset of the Haiti data shows an example of a common point selected (in center) between the optical image (**Left**: OBC) and the LiDAR intensity image (**Right**: Haiti LiDAR Intensity Image). Points should be selected that are clearly identifiable and do not have variation in surrounding height values.

Once all the common registration points were measured in a pattern that covers the image and dense enough for sufficient redundancy to solve the adjustment parameters (see Figure 17 for example of a sufficient pattern), the control point X and Y (Latitude and Longitude if working in geographical space) were derived from the LiDAR intensity image. This was accomplished by performing a single image triangulation adjustment with the image parameters held fixed and the Z ground space coordinate held fixed. The Z height value is an arbitrary value at this point and it does not matter what the value is because the LiDAR intensity image is an orthoimage.

After the initial X and Y values for the control points were determined from this first triangulation solution, the Z height value was updated using the control point editor. The correct Z height value was determined by turning on a terrain tracking tool, selecting the LiDAR DEM as the base terrain layer, systematically visiting each control point X

and Y location, and recording the Z height value. This step completed the creation of full X,Y,Z control points to be used to register the OBC image.

The final triangulation solution that adjusted the OBC imagery using the rigorous panoramic math model parameters produced alignment to the LiDAR point cloud data with marginally acceptable accuracy (Figure 17). The Root Mean Square (RMS) of the ground residuals was 1.9 meters with the longest residual at 3.0 meters. This corresponds to several pixels of misalignment for the image and LiDAR data.

Previous to this research, investigation had been done to develop more robust and user friendly support data for OBC imagery that would have more utility and be able to be used across many software packages, not just Socet Set. Success had been achieved in computing RPC support data for each segment, which made exploitation much easier. An added benefit surfaced as a result of the comparisons between the rigorous model support data and the RPC support data. The added benefit of the RPC support data was that when the RPC adjustable parameters were used to adjust the imagery, a better fit to control was achieved.

Because of this previous, unpublished knowledge, RPC support data was generated for the Haiti segment using the Socet Set "fast sensor model" and "image chipping tool." The same control point selection approach was then used to register OBC to the LiDAR with very good results (Figure 17). The RMS of the ground residuals improved to 0.5 meters with the longest ground residual at 1.1 meters.
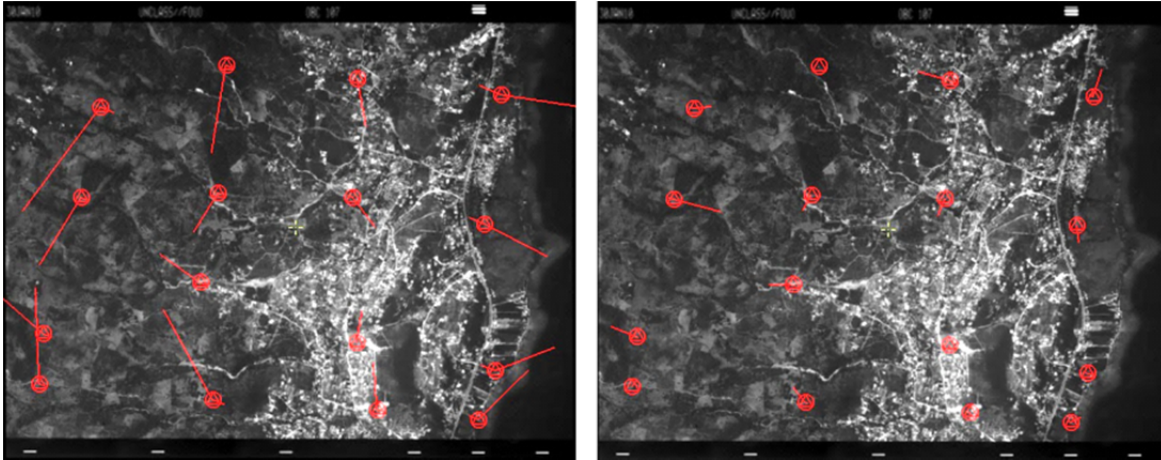
Figure 17.   These base images for Haiti show a scanned segment of an OBC image
and the control point locations (red circle with red diamond) with red vectors.
The **Left** image shows ground space residuals as a result of the rigorous
panoramic model adjustment. (**Left: RMS 1.9 meters**)
The **Right** image shows the improved ground space residuals as a result of using
the RPC adjustment (**Right: RMS 0.5 meters**). **Scale:** Longest vector is 1.1
meters on the right image.

Following this RPC parameter adjustment aligning the OBC imagery to the
LiDAR point cloud, an orthorectification of the OBC imagery was performed using the
adjusted RPC parameters and the LiDAR DEM. QT Modeler software was then used to
merge the LiDAR point cloud and the OBC orthophoto in a fusion process. The process
in QT Modeler simply imports the LiDAR data and then adds the orthophoto as texture.
Internal to QT Modeler, the LiDAR data is stored as individual XYZ points with each
point receiving the added attribute of a Red-Green-Blue (RGB) value derived from the
OBC orthophoto at that pixel location. The following figure (Figure 18) shows the
results of the LiDAR point cloud and OBC image fusion using QT Modeler.
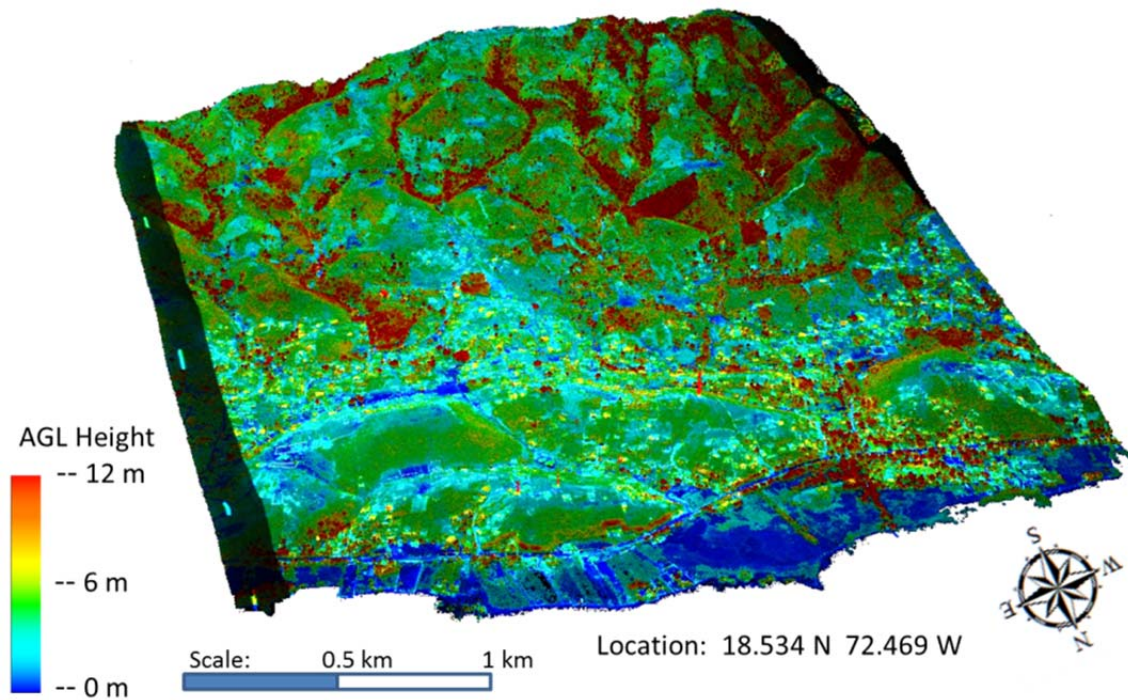
Figure 18.   OBC image and LiDAR point cloud fusion showing the complete registered image. LiDAR points are color coded by Above Ground Level (AGL) height where AGL = DSM – DEM.

The following figure (Figure 19) shows a detailed perspective view using QT Modeler to display the LiDAR point cloud with the OBC image used as texture for the points.
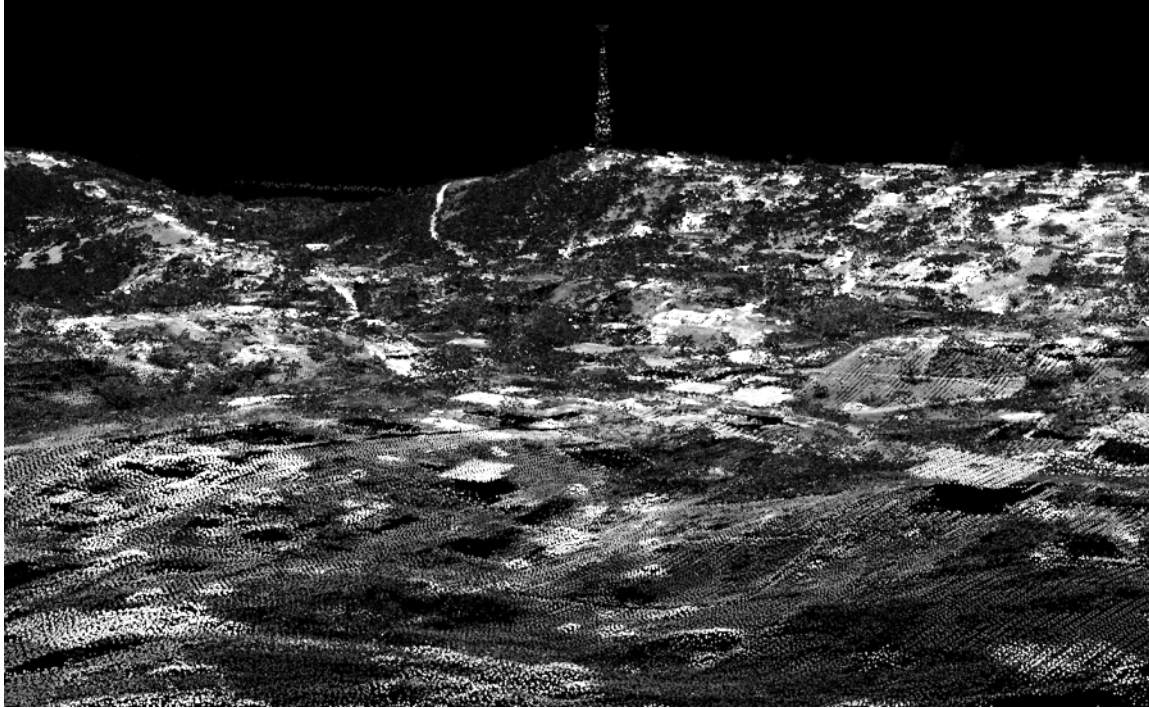
Figure 19.   Haiti LiDAR data with the registered OBC used as
texture for the points

Figure 19 demonstrates that the building tops appear to have good alignment and that the road and tower on the hill also have good alignment with the OBC image texture. Individual points from the point cloud can also be seen on the figure.

2.   NPS Campus LiDAR and High Resolution Aerial Imagery

The NPS Campus LiDAR and High Resolution Aerial Imagery were collected in conjunction with precision GPS and INS/IMU data to meet accuracy requirements. Because of this accuracy requirement, no registration was performed to adjust the imagery to the LiDAR point cloud data.

3.   San Diego LiDAR and WorldView 1 Imagery

The WV1 stereo image registration to LiDAR used the same LiDAR "Intensity Image" and LiDAR DEM interpolation technique to create control points that were used in a WV1 only triangulation process. Refer to Table 1 above for the high level process

flow. The following diagram shows the location of the control points in the area of the LiDAR data set.
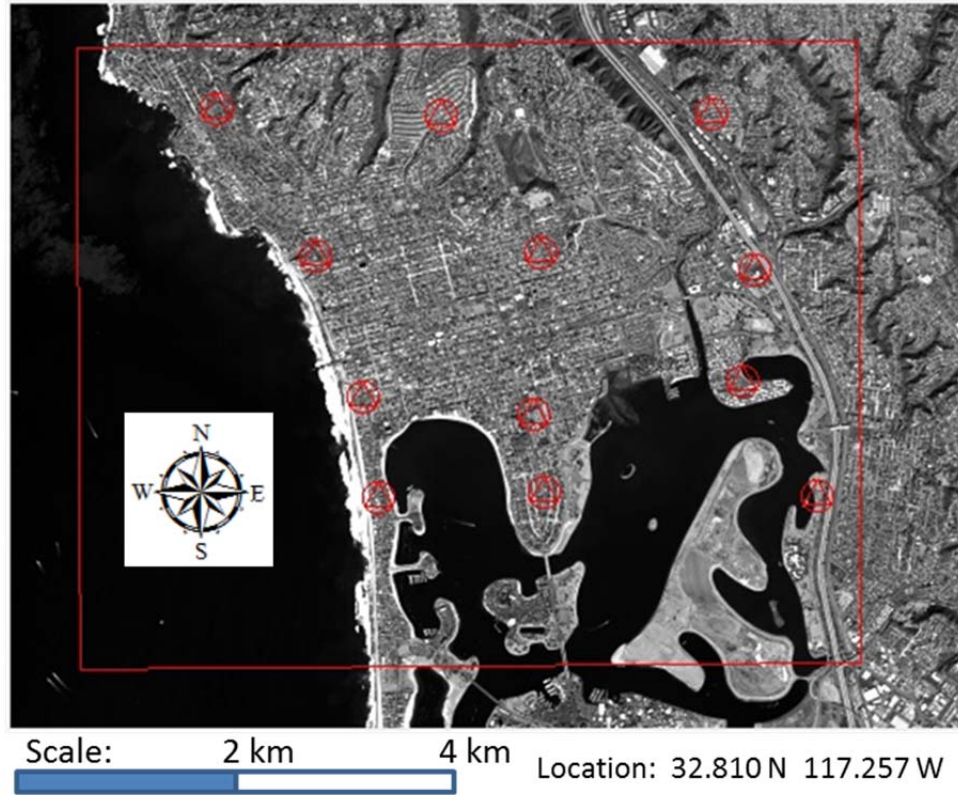
Figure 20. WV1 background image (image 214) showing the location of the LiDAR boundary in red together with the location of the control points (12 points identified as red triangles within red circles)

Control points on the LiDAR intensity image were selected in relatively flat, elevation homogeneous regions. Many of the points were small, flat features in the center areas on roof tops as this test area was primarily urban. The following example shows the selection of a control point on a street marking. Generally, painted street markings do not make good image to image registration control points because they can change or be moved slightly over a short time span. This one appeared to be relatively unchanged.

Figure 21. This side-by-side image display shows an example of a common point selected (center red crosshair) between the optical image (Left: WV1) and the LiDAR intensity image (Right: Pacific Beach LiDAR Intensity Image). Points should be selected that are clearly identifiable and have very little variation in surrounding height values

Once all the control points are selected, the horizontal ground coordinates for the points on the intensity image must be computed. For the purposes of this research, this was accomplished using the Socet Set solve routine and adjusting only the X and Y value of the point. It could also be computed in other software using similar approaches. The image position parameters are "locked" and the Z coordinate (meaningless in this initial adjustment) is also "locked." Running the solve with these settings and only the intensity image active will give precise horizontal coordinates for the points that now become control points.

The vertical control value is arrived at through interpolation of the LiDAR DEM, as the point that has been created does not coincide with a real point in the LiDAR point cloud. In Socet Set, this can be accomplished by turning on terrain tracking with the LiDAR DEM selected and systematically visiting each point. Similar approaches can be used in other software. This will allow interpolation of a Z value for the visited control X,Y location. These interpolated Z values now become the precise vertical control location.

The final controlling adjustment on the WV1 stereo images is performed using these control points and a normal, WV1 only adjustment. Results of this adjustment were very good as shown in Figure 22. Ground control points fit to an RMS of 0.6 meters.
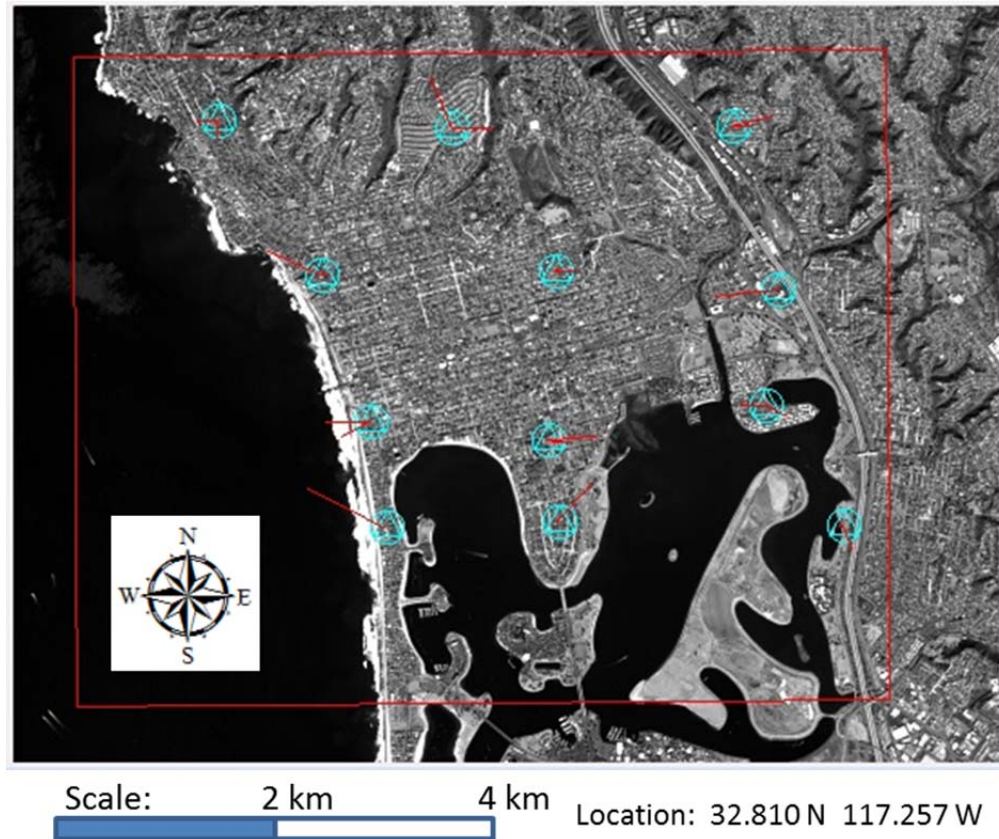
Figure 22.   WV1 background image showing ground space residual analysis results
of the triangulation adjustment that controlled the
WV-1 stereo triplet to the LiDAR data. The RMS was 0.6 meters

C.   STEREO IMAGE POINT CLOUD EXTRACTION

The next critical step in this process was to extract a digital surface model (DSM) from the stereo images. Socet Set has an automated dense terrain extraction tool called the Next Generation Automated Terrain Extraction (NGATE) tool. NGATE has many features that allow dense DSMs to be automatically measured that resemble a LiDAR point cloud. One feature is the interpolated estimate or starting point of adjacent points. The software will use surrounding point correlation information to better predict the height to try an auto-correlated measurement. A second feature is the ability of the

software to take advantage of multiple (more than 2) perspective views of a single point. This can work well around buildings and occluded objects. It should be possible to use similar approaches to obtain similar results using other DSM-generation software.

1. Haiti Site (OBC)

No stereo data were available for the Haiti site, thus a stereo point cloud was not attempted.

2. NPS Campus Stereo Imagery

The NPS campus stereo imagery is very good quality photogrammetric imagery as reported by the WSI report (Watershed Sciences, 2012) and as shown in Figure 8 and Figure 9 above. The stereo pair that covered the "774" subset of the NPS campus area was image id 105 and 106. These images have an average of 0.12 meters ground sample distance (GSD). NGATE was set up to produce a grid spacing equal to that of the LiDAR collection at 0.15 meters. The following figure (Figure 23) shows an example of the DEM grid spacing. Even though this is a very small area, the DEM grid contains 4,020,025 posts. Every fifth post has been displayed in order to see the grid better.

Figure 23.   Portion of the DEM grid (every 5th post displayed) near Herrmann Hall
on the NPS campus showing the density of the grid
(0.15 meter point spacing)

Fortunately, the NGATE software in Socet Set will attempt autocorrelation on all
points as it would be virtually impossible to edit each point manually. The results of the
collected NGATE autocorrelation DEM is shown in Figure 24. It should be possible to
generate similar results using other autocorrelation software.
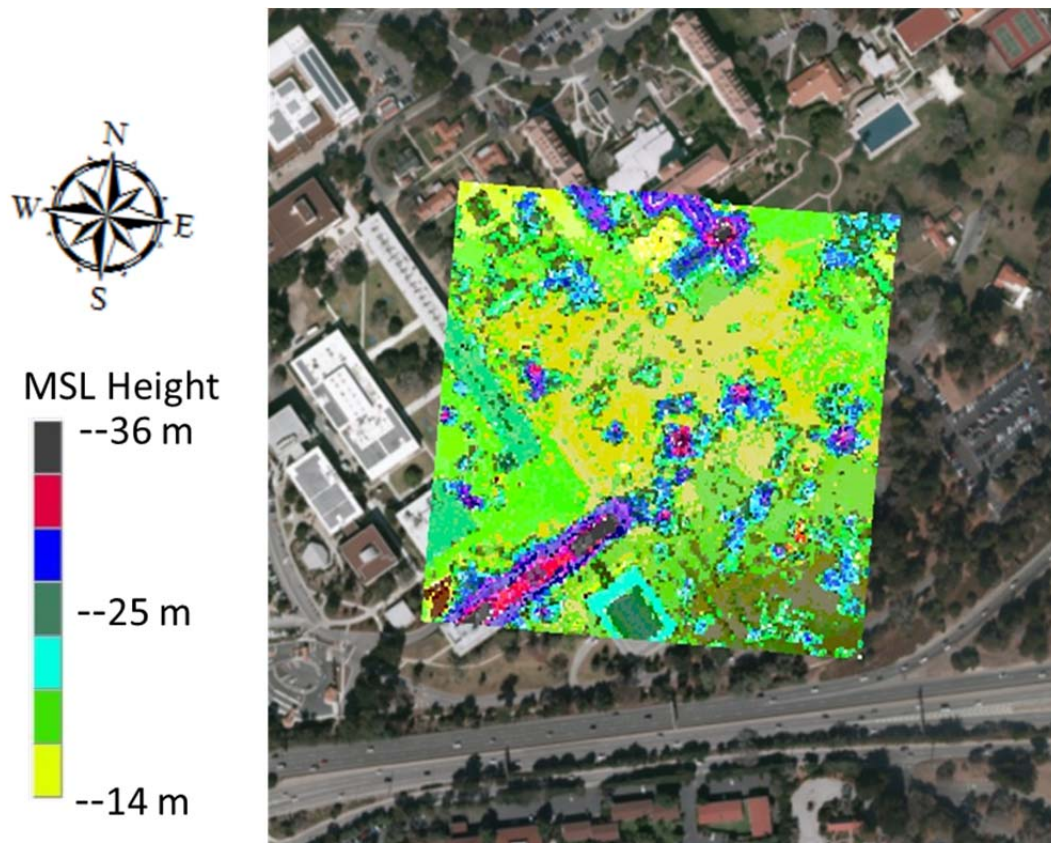
Figure 24. High density DEM (0.15 meter point spacing) over NPS campus
auto collected from stereo pair 105/106 using Socet Set NGATE software
(4,020,025 total points). These data were be used for LiDAR/Optical fusion.
MSL = Mean Sea Level heights (MSL = Ellipsoid Height – Geoid Separation)

The next step in the process was to take the high density DEM and convert it to a point cloud. This was accomplished by exporting the DEM from Socet Set as an ASCII grid file and importing the ASCII grid file into QT Modeler as a point cloud. The following figure (Figure 25) shows the high density collected DEM converted to a point cloud. Other software should be able to achieve similar results.
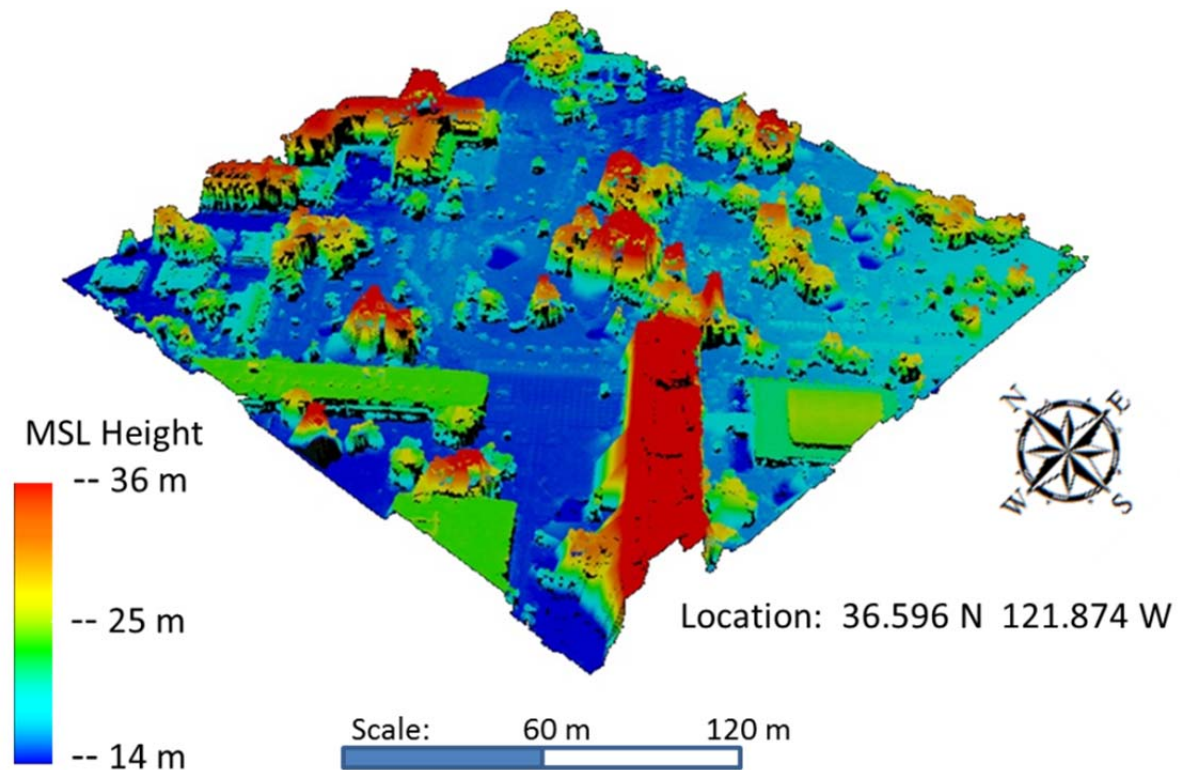
Figure 25.   High density DEM (0.15 m. post spacing) imported into QT Modeler
as a point cloud to be used for LiDAR fusion.

At first, it appeared as though there were too many errors around the trees and near the building edges of the NGATE autocorrelation. The auto-correlated points in the tree and building edge areas seemed to be interpolated and of poor quality. Including 3 images (104/105/106) in the stereo extraction was attempted to aid in precise autocorrelation. The results did not, however, improve the stereo point cloud as well as expected (Figure 26). Many autocorrelation errors still existed. The autocorrelation errors were also affected by sun shadows even though these images were all shot within tens of seconds of each other, and the shadows did not change.

MSL Height

--36 m

--25 m

--14 m

Scale: 100 m   200 m

Location: 36.596 N 121.874 W
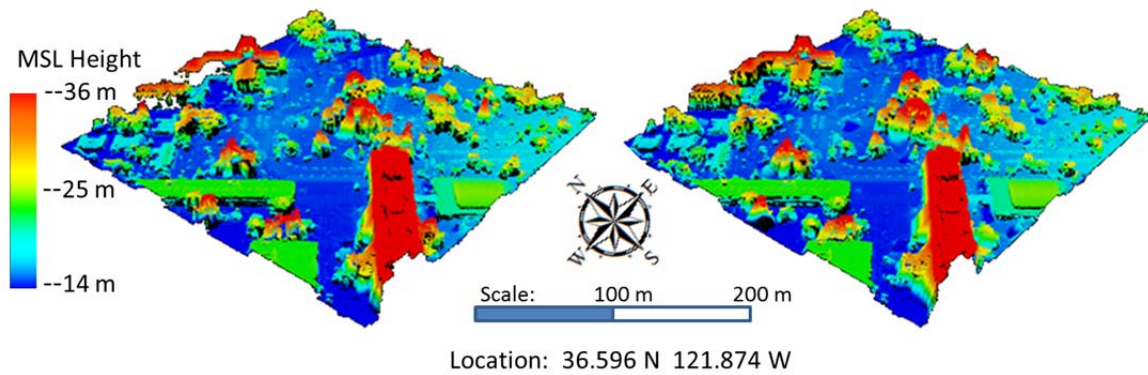
Figure 26.   Side by side view showing the difference between a 3-photo stereo extraction (Left Image) and a 2-photo stereo extraction (Right Image). Autocorrelation errors exist (10 meters) around trees and near building edges in both images with no discernible advantage for either method.

The two photo stereo point cloud was considered acceptable for use in the LiDAR fusion process because all other stereo image autocorrelation results were similar. A realization did surface from this experiment. It was concluded that any level of stereo DEM extraction would contain errors. The consequence is that the data have to be manually edited by measuring each point individually or using tools to edit points as a group. This can be extremely time consuming and expensive. The alternative is to accept the errors, and use the data in the unedited state—pure autocorrelation data—which is the path that I chose for this research.

3.   San Diego WV-1 Stereo Imagery

The WV-1 stereo imagery over the San Diego area (Figure 12 and Figure 13 above) was collected as what is called a stereo triplet. This stereo triplet is three images collected consecutively in the same orbital pass over an area. WV-1 imagery when collected has absolute position capability to 6 meters 90% of the time and each image is independent. The fact that the images are independent implies that the stereo pairs will have parallax that must be removed. This removal of parallax and the absolute positioning improvement was accomplished in one step when all three WV-1 images were registered to the LiDAR data (Figure 22 above). The following figure (Figure 27) shows the perspective views of the stereo triplet.
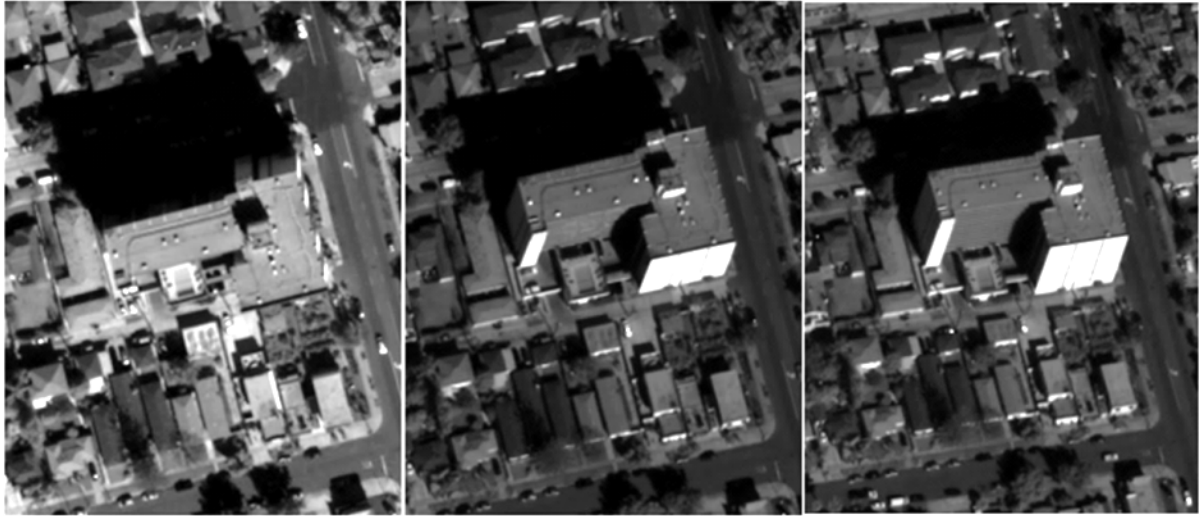
Figure 27.   Side by side display of the WV-1 triplet zoomed in on a prominent
building feature. The images were collected during the same orbital pass
on 08 Feb 2009. From left to right the image id's are 139, 214, and 228

Images 214 and 228 were chosen for stereo image DEM extraction because the perspective views were similar resulting in less occluded features.   Figure 27 demonstrates that image 139 has a perspective view that is completely different than image 214 and 228.   Using image 139 with any other image would prove to be very difficult for the autocorrelation routine.

The grid spacing for the WV-1 stereo image extracted DEM was set similar to the LiDAR data point spacing at 1.4 points per meter. This translated into approximately 0.8 meter equivalent grid spacing for the DEM. This is about the resolution of the WV-1 imagery at 0.7 meter GSD. The following figure (Figure 28) shows the DEM grid displayed over the WV-1 image (every 5th point has been displayed for clarity).
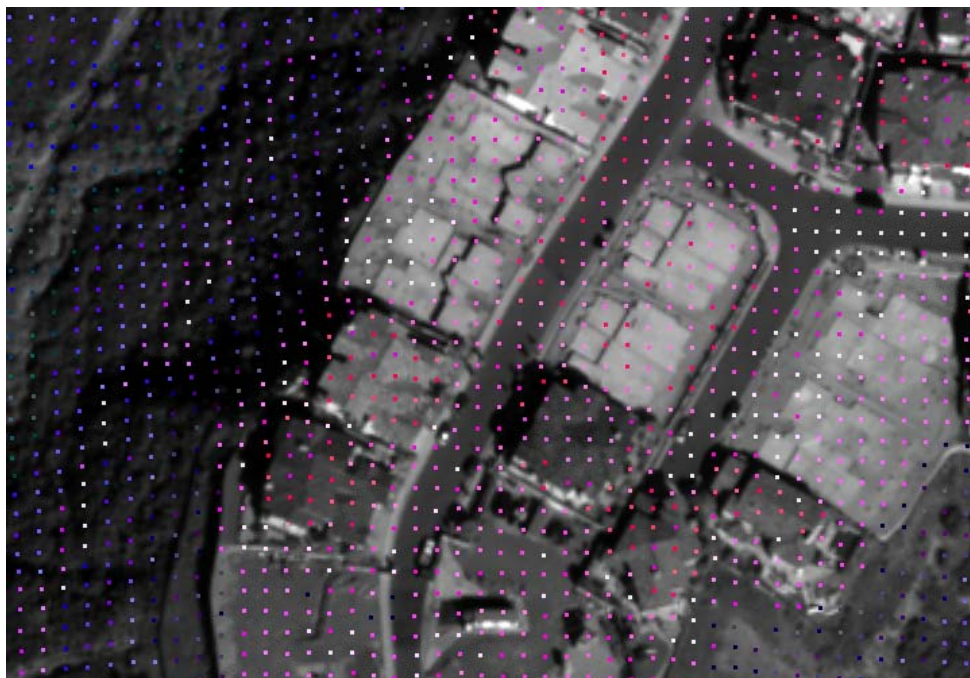
Figure 28.   Portion of the WV-1 stereo derived DEM grid (every 5th post displayed) showing the density of the grid (0.8 meter point spacing)

The complete collection of the Socet Set NGATE automatic DEM point extraction is shown in the following figure (Figure 29).
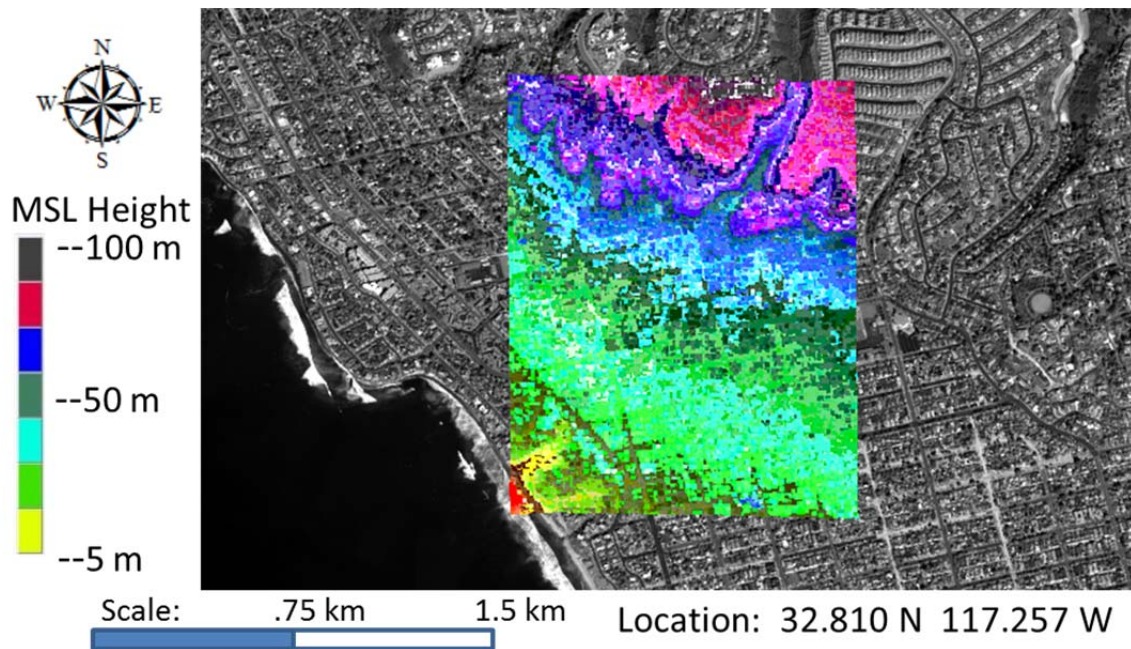
Figure 29.   WV-1 stereo pair collected DEM (0.8 meter point spacing) auto
collected from stereo pair 214/228 using Socet Set NGATE software
(2,141,400 total points).

The next step in the process was to take this stereo derived WV-1 DEM and generate a point cloud. This was accomplished by exporting the point cloud as an American Standard Code for Information Interchange (ASCII) DEM and importing this ASCII DEM into QT Modeler as a point cloud. The following figure (Figure 30) shows a display of that point cloud.
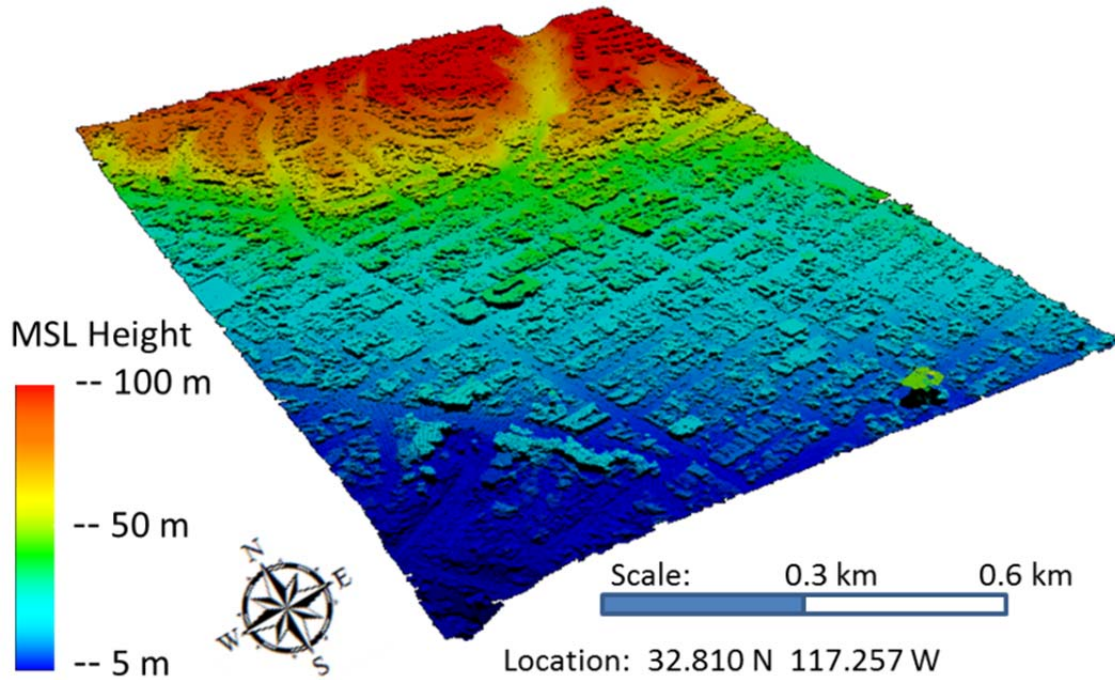
Figure 30.   WV-1 stereo derived DEM converted to a point cloud to be used
for LiDAR fusion.

Similar to the high resolution image DEM extraction from aerial photographs, the WV-1 point cloud has many errors near building edges and near trees. No manual editing was performed and the data were used as a pure autocorrelation data set. At this juncture, the DEM point cloud data was ready for LiDAR fusion.

D.   CHANGE DETECTION USING LIDAR AND STEREO POINT CLOUDS

Fusion of LiDAR point cloud data and stereo point cloud data has many applications as outlined in the Introduction and Background chapters of this thesis. This research focused on two of those applications in the form of point cloud change detection and a fused Image-LiDAR product capable of measuring precision 3D coordinates. For change detection to occur, the LiDAR point cloud and stereo image point cloud data sources must be coincident. The previous sections in this thesis highlight methods to achieve this coincidental alignment by using the LiDAR intensity image and LiDAR DEM as a control source for the stereo imagery. The registration of the stereo imagery to the LiDAR data results in a stereo derived DEM that is coincident with the LiDAR point cloud.

42

Change detection can be an important tool to rapidly assess damage due to a natural or man-made event. Natural events like hurricanes, earthquakes, tsunamis, or fires can be assessed with before event and after event feature level data like a LiDAR point cloud or stereo derived point cloud. The following examples of the NPS campus data and the Pacific Beach data demonstrate how change detection can be used for analysis in spite of potential noise in the data sets.

1. NPS Campus LiDAR and Stereo point cloud change detection

Before beginning the change analysis, it was important to inspect and visualize the data. The following figure (Figure 31) show a side-by-side view of the LiDAR point cloud and the Stereo point cloud for comparison of quality.
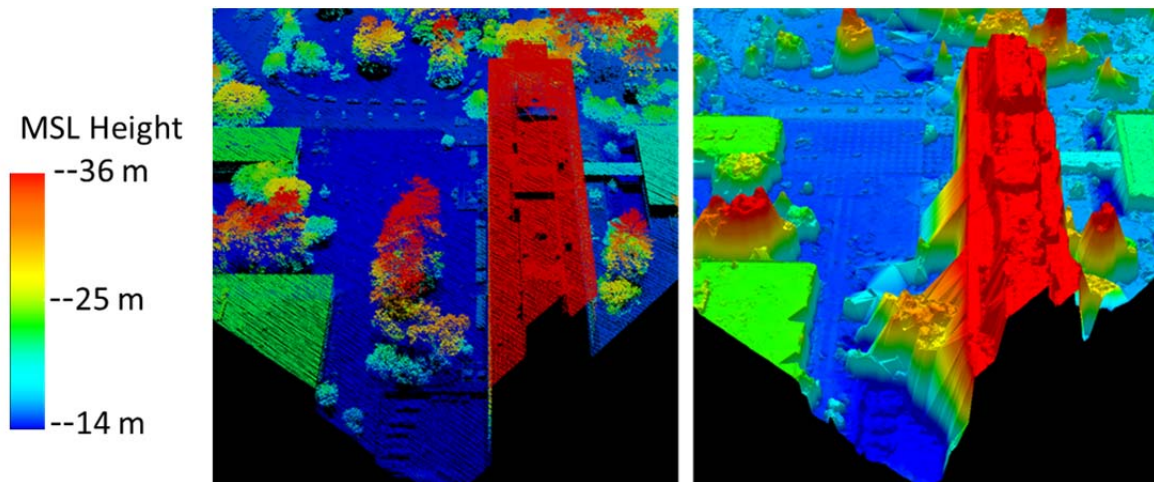
Figure 31.   Split screen close up view of the LiDAR data on the left and the stereo image collected point cloud on the right showing many unique differences. The LiDAR data is very clean and sharp (Left) and the Stereo point cloud is interpolated and rough in areas (Right).

It proved to be very difficult to get a good, clean point cloud from the optical imagery even though the imagery was high quality. Notice how well the LiDAR point cloud data modeled the trees as can be seen by the realistic display of the tree in the center of the left image of Figure 31. Also, notice how clean the building corner lines are for the LiDAR (Figure 31, center red building on left image) and how noisy and sometimes interpolated the building lines are in the stereo cloud (Figure 31, center red

building on right image). Stereo image autocorrelation in tree canopy is very challenging. As was mentioned before, the stereo point cloud data was not manually edited but used as a pure autocorrelation data set.

The next step was to come up with a method to compare these two data sets for change detection in spite of the differences already noticed from the autocorrelation errors. A straight subtraction method was used (data set 1 minus data set 2) to create a new point cloud model for display and analysis. Figure 32 shows the results of the new point cloud created by subtracting the LiDAR point cloud from the stereo point cloud.
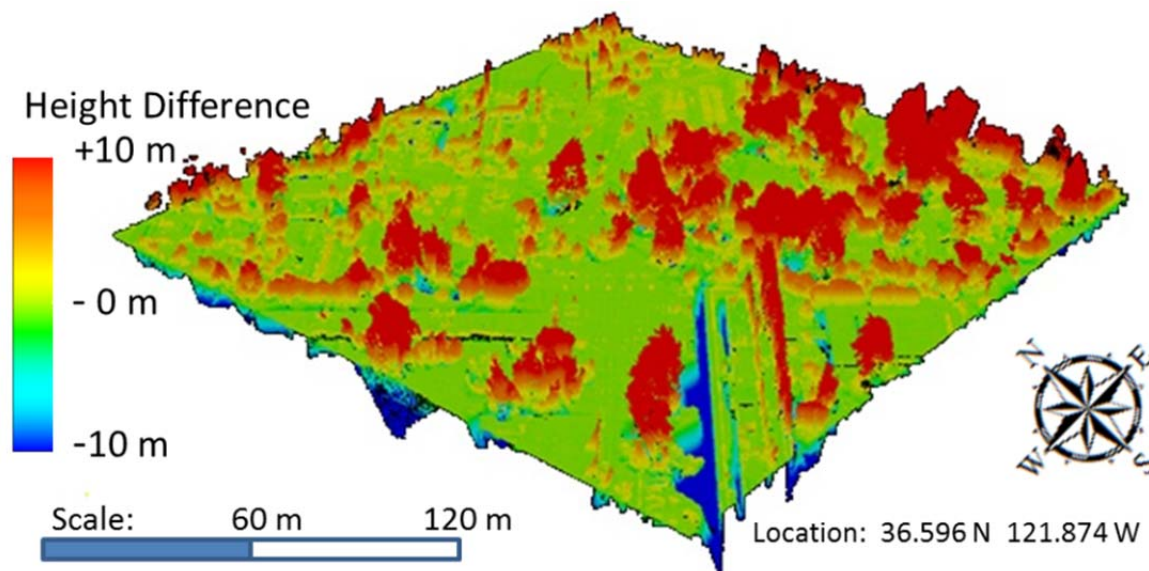
Figure 32. Difference between the WSI LiDAR and Stereo Imagery point cloud Mean: -0.5m; Std Dev: 6.3m; Max: 44.0m; Min: -30.7m

Results appear very noisy but predictable. The trees and building edges have the most noticeable differences as indicated by the red and blue coloration. Even though the differences look catastrophic, there are some good things in here. For instance, building tops, like the ground surface, have not changed.

The results of the autocorrelation and the errors that could potentially exist on either data set required approaching the problem from a different perspective. Instead of focusing on the differences, focusing on the things that stayed the same seemed like a better approach. A high percentage of the autocorrelation data was very good with

autocorrelation performing well on the ground features and building tops. The new approach strategy was to keep the data that were similar and eliminate the noisy outlier data. While there are a number of ways to implement this, the above approach was accomplished for this research by using software called Cloud Compare (CloudCompare, 2004) and clipping the difference cloud that was created in QT Modeler. The following figure (Figure 33) is a visualization of the original difference cloud in the Cloud Compare software.
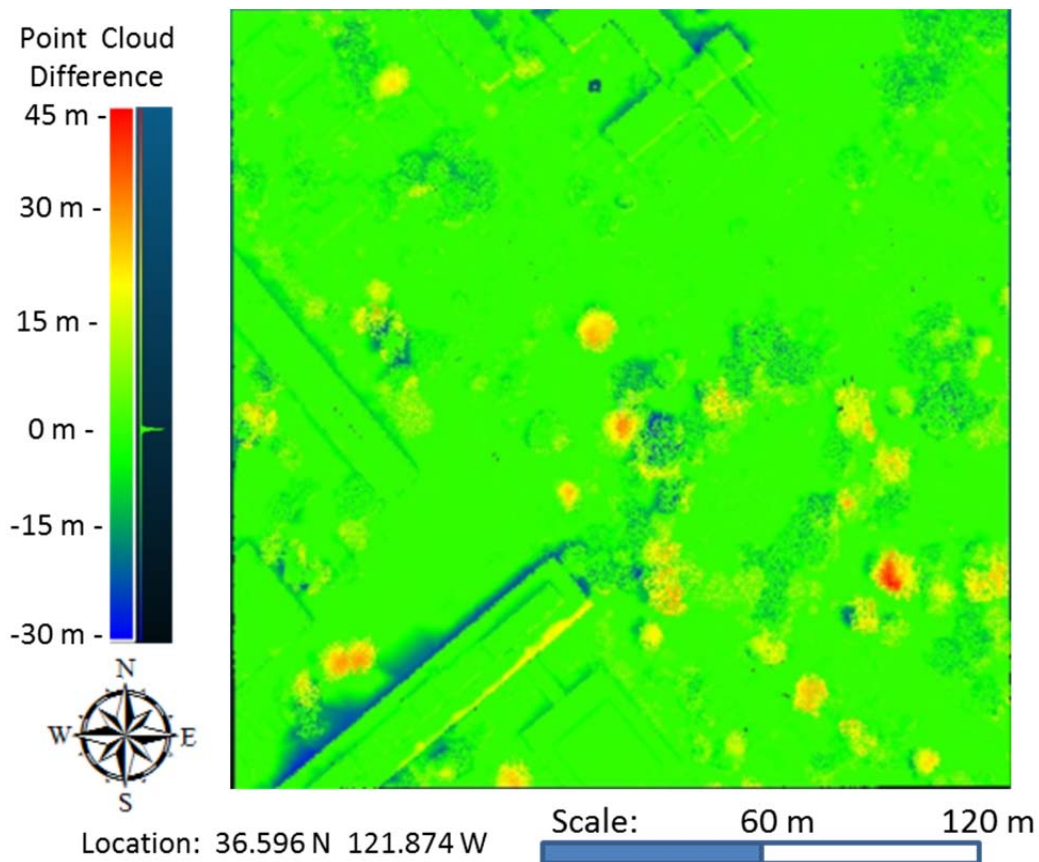
Figure 33.   Vertical display of the point cloud created from the difference between the NPS WSI LiDAR and the Stereo Image autocorrelation point cloud using Cloud Compare (CC) software.

Notice how the majority of the cloud differences shown in figure 33 are near zero (green). The analysis focused on how much of the scene stayed the same and used a difference histogram to capture the statistics. The scale bar shows the height difference

values (in meters) compared to the colors. A small, "on edge" vertical histogram to the right of the scale bar highlights the fact that a majority of the differences are biased by about one meter.

The following figure (Figure 34) represents only those objects that remain the same. The technique is to remove the change outliers, keeping only things that stayed in the same location. The change outliers are extreme differences caused by stereo model auto-correlation inaccuracies, sensor perspective differences, and normal time variant change (cars, building construction, tree removal, etc.).
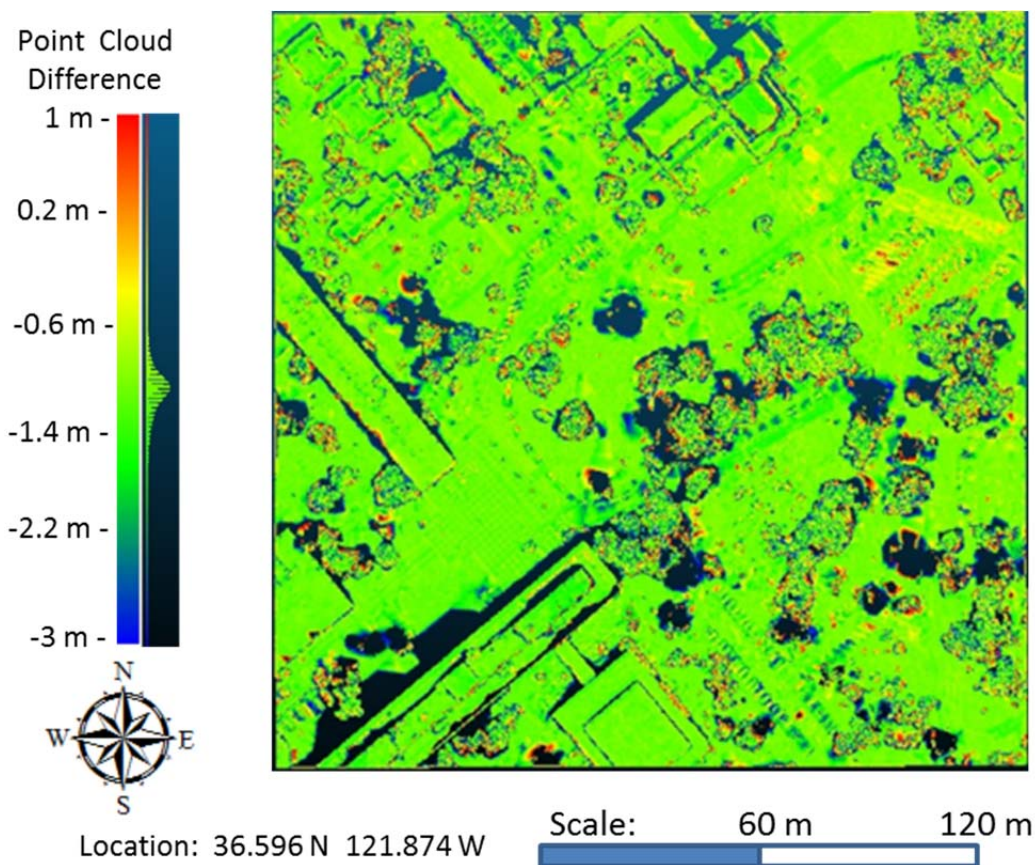
Figure 34.   Display of the first cut edit of the difference data clipped at plus and
minus 2 meters to remove large outliers. The "holes" in the data are
where outlier errors have been removed.

The color image and color scale bar show how much things are the same between the LiDAR point cloud and the Stereo Image derived point cloud. The difference data

have been clipped at plus and minus 2 meters from the mean to remove the outliers. The "holes" are where the outliers existed. Amazingly, 34% of the points have been clipped but the contents of the scene are still discernible (Figure 34).

By further clipping the outlier free data using the statistical 95% confidence interval equation (mean plus or minus two times the standard deviation), subtle differences are detected – almost at the sensor characteristic level.
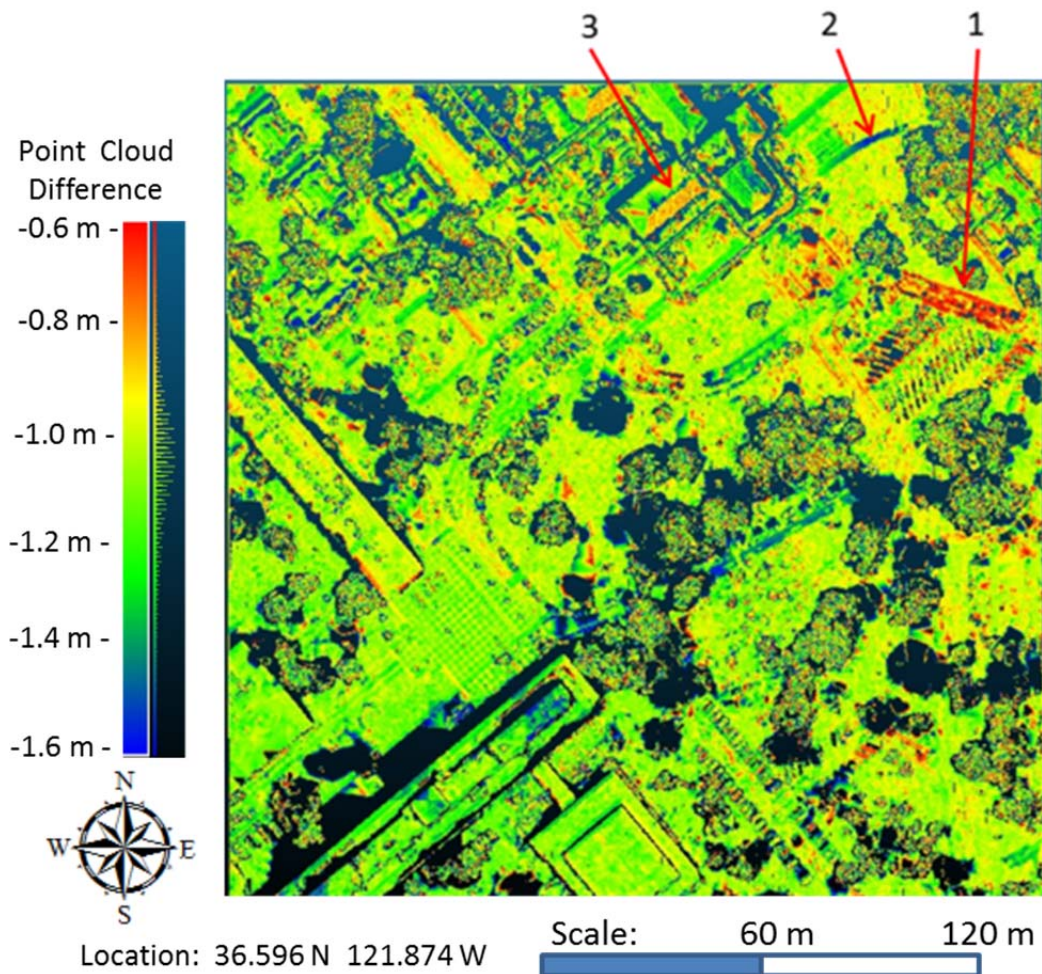
Figure 35.   Display of the difference data after further clipping at the
95% confidence level. The differences are on the order
of 50 cm (.5 meters) from the mean and show peculiar sensor collection
level artifacts (red and blue areas).

In Figure 35, notice the 50 cm difference (red) in the driveway on the upper right of the image (Location 1 identified with the red arrow). Next, there is a -50 cm difference (blue) in the walkway on extreme upper right of the image (Location 2 identified with the red arrow). Notice that the southeast facing roof sections of buildings show a 50 cm difference (Location 3 identified with the red arrow). These are all examples of extremely small differences that are sensor collection dependent or stereo extraction dependent.

The important point is that the buildings and many of the trees remained the same even though quite a bit of noise due to errors in stereo correlation existed. Focusing on things that remained the same by clipping the gross error outliers has allowed analysis to take place at whatever level the errors exist at. The data showed that no extreme differences had occurred. The interesting thing about this analysis was that the final clipped difference data set (90% confidence interval) was able to find differences at the sensor collection level.

2.   San Diego LiDAR and Stereo WV1 point cloud change detection

Visualization and inspection of the data was performed in a similar fashion to that performed with the NPS data. The following figure (Figure 37) shows a side-by-side comparison of the LiDAR point cloud and WV-1 stereo extracted point cloud.
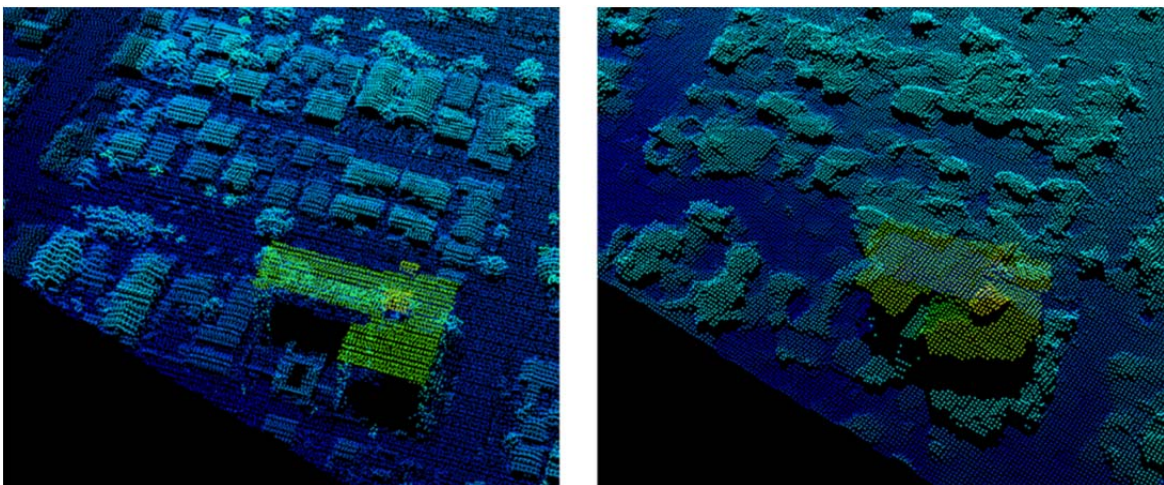
Figure 36.   Side-by-side zoomed in view of the Pacific Beach, CA,
LiDAR point cloud (left) and WV-1 stereo point cloud (right).

The LiDAR point cloud is clean and sharp while the stereo point cloud shows areas of interpolation and missing features. As rough as the WV-1 stereo extracted point cloud was, it was used as a pure autocorrelation data set in the following analysis.

The following figure (Figure 38) is the "first cut" removal of the outliers using a plus and minus 10 foot threshold around the approximate minus 4 foot bias. Fifteen percent (15%) of the point have been clipped as a result of this outlier removal, what remains are things that have not changed dramatically.
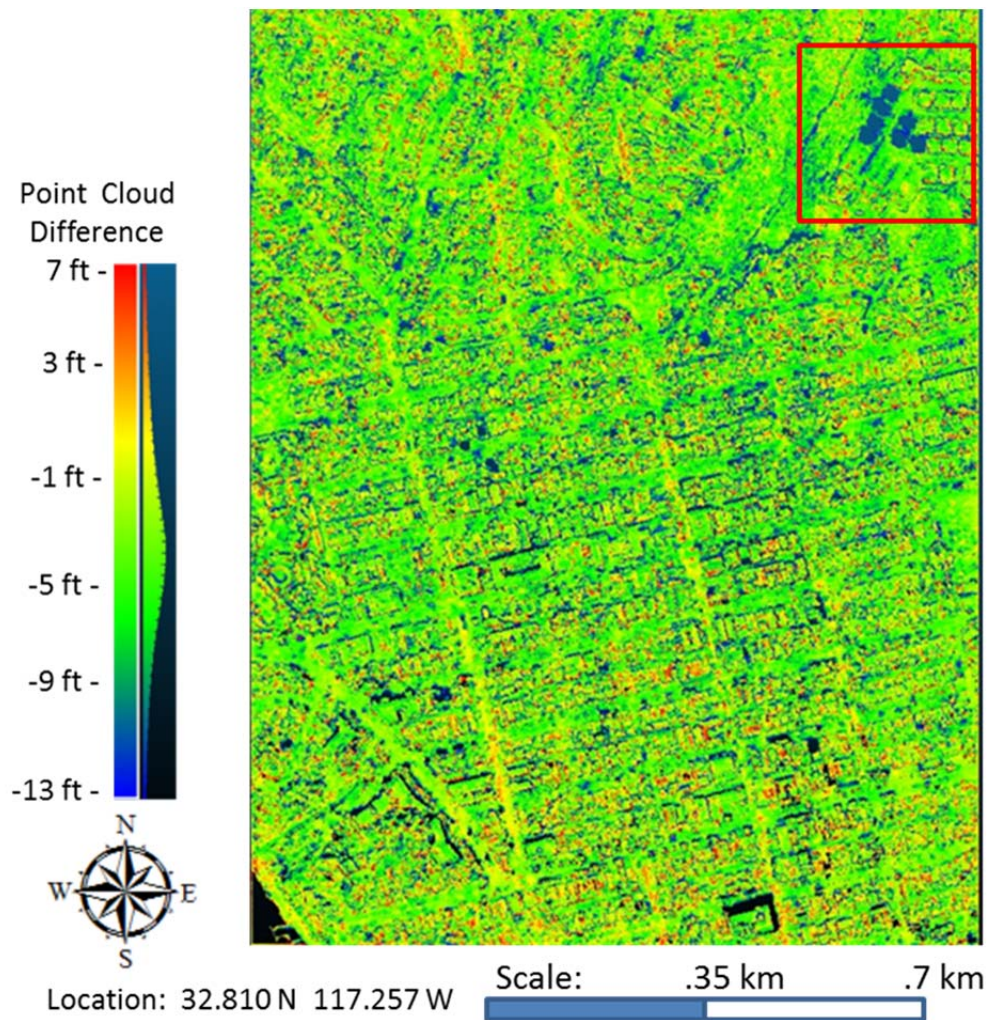
Figure 37.   Cloud Compare software created figure of the entire
Pacific Beach, CA, point cloud comparison test area
showing the results of the "first cut" removal of
difference outliers (85% unchanged, 15% change outlier).

Focusing on the difference data that did not change with the San Diego LiDAR and WV-1 stereo imagery presented an unexpected surprise. The outlier and 90% confidence interval clipping process detected an area of large scale change that corresponded to new home construction during the time of the LiDAR collection (2005) and the WV-1 stereo image collection (2008) (Figure 37). The area that has changed, in the upper right corner, stands out very noticeably as rectangular blue areas (Figure 37, red box). This is seen more clearly in Figure 38. It is easy to pick out the 7 houses in the upper right corner of Figure 37 and central part of Figure 38 that have been built between the 2005 to 2008 time frame (normal – time variant – change). Notice that even with the predominant noise around the homes and in the tree areas, the real change is easily noticeable as large "holes" in the data. It is also easy to pick out the taller building structures because of the auto-correlation outliers along the building edges that have been removed.
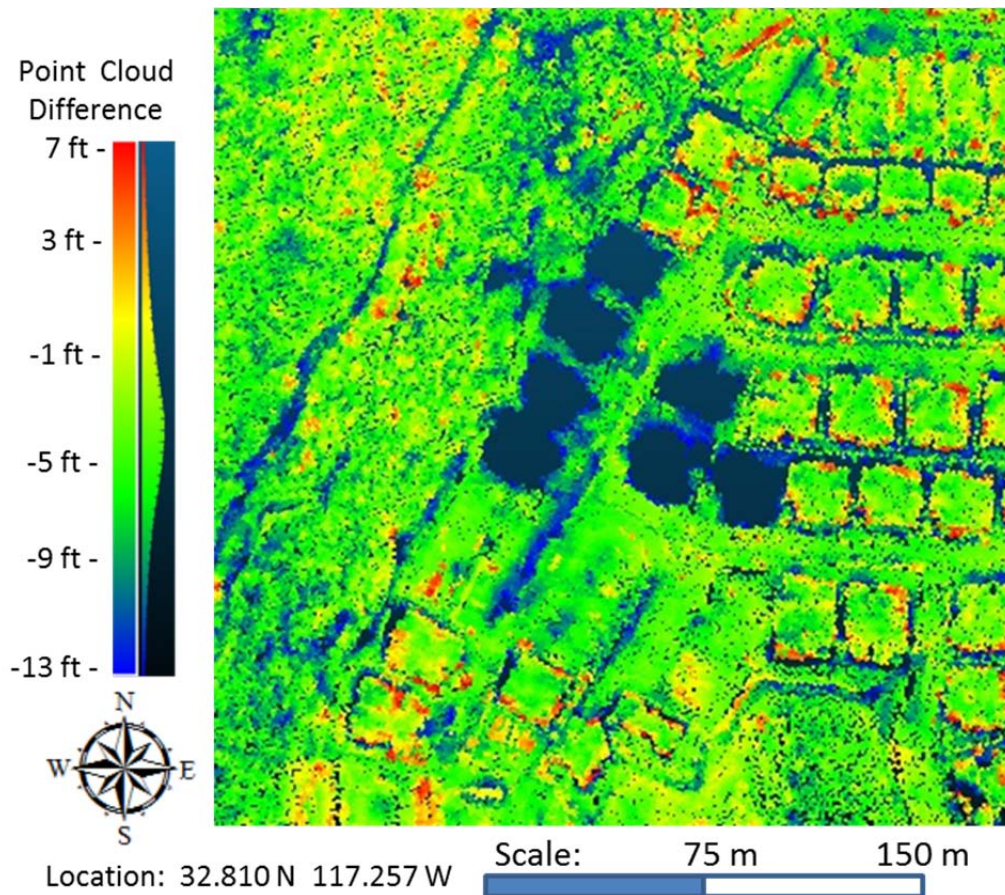
Figure 38. A closer inspection of the new home construction showing the
results of the "first cut" outlier removal. The "holes" in the
data show where new homes were built.

The detection of this new home construction was unexpected and did show that
the outlier removal process does work to detect large scale change. The key is to focus
on the things that stayed the same, clip out the noise, and what you are left with is a data
set that can show large change if it exists.

E.   PRECISION IMAGERY-LIDAR FUSED PRODUCT

The next logical step is to focus on selected aspects of creating a fused optical
image and LiDAR data product viable for extraction of precision 3D coordinates. This is
different than assigning a Red-Green-Blue (RGB) value to each LiDAR point as is
commonly done with LiDAR visualization tools and is supported by the standardized
LiDAR file format (.las). This concept is innovative in that the idea is to preserve the

perspective view of the image, preserve the native resolution of the image, and use the coincident LiDAR data to facilitate precision 3D coordinate extraction (Rodarmel et al., 2006).

The best way to approach this concept is to first build a stereo image base layer that has been registered to LiDAR. The reverse of this can be done, which would be registering the LiDAR to the base layer if the stereo image base layer is considered to be more accurate. In either case, a stereo image base layer and LiDAR data set should exist and should be registered such that they are coincident. Having these two data sets coincident provide for many, very attractive options.

One option is that LiDAR data can be converted to a high resolution DEM and displayed, as individual points, in the stereo imagery. This provides measurable quality assurance for the LiDAR data as well as the stereo image models.

A second option is that if the stereo imagery has a stated accuracy, the LiDAR data accuracy can be either verified or computed. For automated accuracy determination, the LiDAR accuracy can be computed by using an autocorrelated stereo image point cloud to LiDAR point cloud change detection process outlined in this thesis. Even with the noise of the stereo autocorrelation, a statistical change can be calculated allowing absolute and relative accuracy to be computed.

In the most likely scenario, a new, more current and detailed image would be collected that would need to be registered to the LiDAR data. In this case, the stereo base layer provides for an attractive auto-registration layer that could be used to adjust the new image. Once coincident with the stereo base layer, the image can then be easily fused with the LiDAR data as it too is coincident with stereo base layer.

V.   SUMMARY

LiDAR point cloud data, imagery, and stereo image derived point cloud data are ideal candidates for data fusion to provide high precision digital elevation models and improve change detection. In order for accurate fusion to occur, however, the LiDAR and imagery must be coincident.

This research demonstrates the importance of registering optical imagery to LiDAR data as a basis for proper, seamless fusion. Several dissimilar image data types were chosen to test optical image to LiDAR registration methods, including an airborne panoramic film image (OBC), high resolution stereo frame color images (UltraCam Eagle), and panchromatic satellite images (WV1). Likewise, several LiDAR sets of varying point densities and quality were chosen including LiDAR of Haiti at 3.4 points/m^2, the NPS Campus at 30.0 points/m^2, and a portion of San Diego, California LiDAR at 1.4 points/m^2.

Individual points in a LiDAR point cloud are not easy to precisely identify on an image, consequently, methods for optical image to LiDAR registration were researched with the realization that the most practical method is to use the LiDAR-derived intensity image as an X,Y (Latitude, Longitude) control base and the LiDAR-derived DEM as the Z or height control base. A logical control point selection method was established that used features that were homogeneous in surrounding height. This helped with extracting a more precise height at a given X,Y location because the height could be interpolated from the LiDAR derived DEM.

A new and robust process for registering optical imagery to LiDAR was developed as part of this research. This new method uses a two-step triangulation process that derives ground control from the LiDAR intensity image in one step and then adjusts the imagery in a second step. The advantages of this new method are that all measured points are fully reviewable and the initial triangulation process provides quality assurance of the intensity image control points.

These new methods and processes were applied to data for three test sites. In the first test scenario, OBC image adjustment to LiDAR for an area in Haiti proved to be problematic using the panoramic math model as the image and control points did not match well (RMS 1.9 meters). A better approach used the RPC representation of the panoramic math model followed by an affine transformation to fit the image to control points, with an improved RMS of 0.5 meters. The well-registered results permitted high resolution visualization of the OBC imagery and Haiti LiDAR point cloud. The RPC adjustment approach should help to streamline future OBC image and LiDAR fusion processing and bring more utility to the OBC imagery, as RPC adjustments are supported by more software packages than rigorous panoramic math models. The OBC imagery was not in stereo (a single image) so no further point cloud analysis was performed with this data set.

Fusion of high resolution optical aerial imagery and dense LiDAR data of a portion of Monterey, California, over NPS campus was very straightforward. This well calibrated imagery had very good positional and attitude information, resulting in precision stereo pairs that needed no triangulation to remove parallax or control points to register the imagery to the LiDAR. The data sets were virtually coincident from the start, resulting in easy fusion of the imagery and LiDAR point cloud. The high resolution nature of the imagery and LiDAR data allowed for excellent 3D visualization of the NPS campus.

For the NPS dataset, a high resolution DEM was automatically collected from the stereo images and this DEM was converted into a point cloud. Several automatic DEM extraction strategies were evaluated in the attempt to create a quality DEM. After these strategy tests, it was realized that autocorrelation errors will always be present and the perfect stereo collected point cloud cannot be obtained from autocorrelation alone.

The NPS LiDAR point cloud and the stereo point cloud were then used as separate entities to create a change detection layer. A new point cloud was created that contained the difference between the LiDAR point cloud and the stereo point cloud. Using this "difference cloud", a unique strategy was devised to focus on things that stayed the same as opposed to focusing on things that were different. This strategy used

a 90% confidence interval bracketing method that clipped outliers and autocorrelation errors. Surprisingly, this method worked well to show that buildings, objects, and trees were generally unchanged even though 30% of the points were noise caused by stereo image autocorrelation errors.

The final test case investigated WV1 stereo image registration to LiDAR data and stereo image derived point cloud versus LiDAR point cloud change detection for the San Diego, California, site. The improved registration process was used to triangulate (remove y-parallax) and register (control) three WV1 images to the LIDAR intensity image and LiDAR DEM resulting in a good registration solution (RMS 0.6 meters).

Following registration of the three WV1 images, several autocorrelation strategies were attempted with the stereo imagery to try to create the perfect point cloud. The best WV1 autocorrelation point cloud, however, was still very noisy. A difference point cloud was created using the 90% confidence interval bracketing method to clip outliers and autocorrelation errors, resulting in detection of unforeseen urban change in the form of new home construction in the image.

A short description of the concepts for creating a fused LiDAR/Image product was presented focusing on the requirement of using an accurate and coincident stereo image base layer as the foundation. Accuracy can be computed for the LiDAR data using the same stereo image point cloud to LiDAR point cloud change detection process outlined in this thesis regardless of the high potential for stereo autocorrelation errors. If a new, more current and higher resolution image is collected, the stereo base layer can be used in a photogrammetric auto-registration routine to align the new image with the stereo imagery with the added result of being coincident with the LiDAR data for easy fusion.

THIS PAGE INTENTIONALLY LEFT BLANK

VI.   CONCLUSIONS

This research focused on demonstrating the processes and techniques of registering photogrammetric imagery to LiDAR point cloud data, and the importance of this registration as the precursor for data fusion. Point cloud data derived from optical stereo images were compared to LiDAR point cloud data and basic change analysis was performed. This work is a precursor to a larger initiative to create a "ready to use" photogrammetric image and LiDAR fused data set.

Most image to LiDAR registration processes utilize edge matching techniques, however, this requires identifiable object edges throughout the image and sophisticated software to identify and extract those edges. The LiDAR intensity image approach demonstrated here proved more capable as it did not require the image to contain object edges which allowed registration of many image types with varying scene content. The intensity image approach was also easily adapted from known image–to–image registration approaches and a new procedure was developed for this process. A unique individual point selection technique that requires the point to be in a homogeneous height area was successful because it minimized the amount of derived LiDAR DEM height interpolation error.

A new, 2-step triangulation process coupled with an RPC math model approach was used to improve the registration of the OBC panoramic imagery to LiDAR data. Significant improvement was achieved, from an RMS of 1.9m using the rigorous model to an RMS of 0.5 meters using the RPC method. The RPC adjustment approach should help to streamline future OBC image and LiDAR fusion processing and bring more utility to the OBC imagery, as RPC adjustments are supported by more software packages than rigorous panoramic math models. For all image types, the 2-step triangulation had the added benefits of retaining registration point measurements for quality review and intermediate control point derivation output for quality assurance.

High resolution DEM extraction from stereo imagery can have as much as 30% autocorrelation failure principally near building edges and tree canopy. This high rate of

error was overcome when performing stereo image and LiDAR point cloud change analysis by clipping the outliers by a 90% confidence interval bracketing method to create a new point cloud by differencing the LiDAR point cloud and the stereo image point cloud. The display and analysis of the difference point cloud resulted in measurable change detection. This technique produced results that detected small scale (<50 cm) differences and unforeseen large scale change in the form of new home construction.

Finally, a concept for a fused image and LiDAR data set was presented that focuses on creating a stereo image base layer that is coincident with the LiDAR data. This concept has many benefits including stereo image and LiDAR accuracy verification, LiDAR accuracy computation, and easier succeeding image/LiDAR registration and fusion. This research and these benefits justified the proposal for a fused LiDAR and stereo base layer as the foundation for further LiDAR/image fusion.

LIST OF REFERENCES

Applied_Imagery. (2004). (Version 8.0.0) [Quick Terrain Modeler Software] Available from www.appliedimagery.com. Silver Springs, MD.

BAE_Systems. (1990). (Version 5.6.0) [Socet Set Software]. San Diego, California.

CloudCompare. (2004). (Version 2.5.0)[Software]. Available from http://www.danielgm.net/cc/.

Du, Q., Xu, B., & Cao, H. (2009). Registration of airborne LiDAR data and aerial images based on straight lines and POS data. *Proc. SPIE 7498, MIPPR 2009: Remote Sensing and GIS Data Processing and Other Applications,* 749835, pp. 1–6.

Habib, A., Ghanma, M., & Kim, E.-M. (2005). Lidar data for photogrammetric georeferencing. *International Federation de Geometres Working Week*, (pp. 1–15). Cairo, Egypt.

Habib, A., Kersting, J., McCaffrey, T., & Jarvis, A. (2008). Integration of lidar and airborne imagery for realistic visualization of 3D urban environments. *International Society of Photogrammetry and Remote Sensing*, 37, pp. 617–623. Beijing, China.

Kaminsky, R. S., Snavely, N., Seitz, S. M., & Szeliski, R. (2009). Alignment of 3D point clouds to overhead images. *Computer Vision and Pattern Recognition*. Seattle, WA: Grail Publications.

Leberl, F., Irschara, A., Pock, T., Meixner, P., Gruber, M., Sholz, S., & Wiechert, A. (2010). Point clouds: lidar versus 3D vision. *Photogrammetric Engineering and Remote Sensing,* 76(10), 1123–1134.

Mishra, R. K., & Zhang, Y. (2012). A review of optical imagery and airborne lidar data registration methods. *The Open Remote Sensing Journal,* 5(1), 54–63.

Open_Topography. (2008, December 3). Open Topography [Data]. Retrieved May 12, 2013, from http://www.opentopography.org/index.php

Pohl, C., & Van Genderen, J. (1998). Review article: multisensor image fusion in remote sensing: concepts, methods and applications. *International Journal of Remote Sensing,* 9(5), 823–854.

Rodarmel, C., Samberg, A., Theiss, H., & Johanesen, T. (2006). A review of the ASPRS guidlines for the reporting of horizontal and vertical accuracies in LIDAR data. *International Archives of Photogrammetry and Remote Sensing spatial Information Sciences.* 36, pp. 34–39. Paris, France: Society for Photogrammetry and Remote Sensing, Saint-Mande, France.

Schenk, T., & Csatho, B. (2003). Fusion of lidar data and aerial imagery for a more complete surface description. *ISPRS International Archives*, 34, pp. 310–317.

Schenk, T., Seo, S., & Csathó, B. (2001). Accuracy study of airborne laser scanning data with photogrammetry. *International Archives of the Photogrammetry, Remote Sensing and Spatial Information Sciences*, 34(3/W4), (pp. 113–118).

Shan, J., & Toth, C. K. (2009). *Topographic laser ranging and scanning*. Boca Raton, FL: CRC Press.

UTC_Aerospace_Systems. (2013). *http://utcaerospacesystems.com/cap/products/Pages/optical-bar-camera.aspx.*

Watershed Sciences, I. (2012). *Monterey Naval Postgraduate School Data Collect*. Portland, OR: Watershed Sciences, Inc.

White, J. C., Wulder, M. A., Vastaranta, M., Coops, N. C., Pitt, D., & Woods, M. (2013). The utility of image-based point clouds for forest inventory: a comparison with airborne laser scanning. *Forests,* 4(3), 518–536.

INITIAL DISTRIBUTION LIST

1. Defense Technical Information Center
    Ft. Belvoir, Virginia

2. Dudley Knox Library
    Naval Postgraduate School
    Monterey, California